Bioorganic Chemistry 83 (2019) 262–276

Contents lists available at ScienceDirect

Bioorganic Chemistry

journal homepage: www.elsevier.com/locate/bioorg

Novel nalidixic acid derivatives targeting topoisomerase II enzyme; Design, synthesis, anticancer activity and effect on cell cycle profile

Omneya M. Khalil[a], Ehab M. Gedawy[a,b,*], Afaf A. El-Malah[a], Mina E. Adly[a]

[a] Pharmaceutical Organic Chemistry Department, Faculty of Pharmacy, Cairo University, Cairo 11562, Egypt
[b] Pharmaceutical Chemistry Department, Faculty of Pharmacy, Badr University In Cairo BUC, Cairo, Egypt

ARTICLE INFO

Keywords:
Nalidixic acid
Synthesis
Design
Anticancer activity
Topoisomerase II enzyme
Cell cycle analysis
Apoptosis

ABSTRACT

Aim: Design and synthesis of novel nalidixic acid derivatives of potent anticancer and topoisomerase II inhibitory activities were our major aim.

Materials & methods: All the newly synthesized nalidixic acid derivatives were submitted to the National Cancer Institute (NCI), Bethesda, USA and were accepted for single dose screening. Further investigation *via* IC_{50} determination of the most potent compound **6a** against K-562 and SR leukemia cell lines. Finally, the topoisomerase II inhibitory activity, the cell cycle analysis and molecular docking of **6a** were performed in order to identify the possible mechanism of the anticancer activity.

Results: Compound **6a** showed interesting selectivity against leukemia especially K-562 and SR subpanels with IC_{50} 35.29 μM and 13.85 μM respectively. Moreover, compound **6a** revealed potent topoisomerase IIα and topoisomerase IIβ inhibitory activity compared with known topoisomerase inhibitors such as doxorubicin and topotecan with IC_{50} 1.30 μM and 0.017 μM respectively. Cell cycle analysis indicated that compound **6a** induced cell cycle arrest at G2-M phase leading to inhibition of cell proliferation and apoptosis. Molecular modeling demonstrated that the potent topoisomerase inhibitory activity of **6a** was due to the interaction with the topoisomerase II enzyme through coordinate bonding with the magnesium ion Mg^{2+}, hydrogen bonding with Asp 545 and arene cation interaction with His 759.

1. Introduction

Topoisomerase II enzyme is a nuclear enzyme that plays crucial functions during DNA processes such as, replication, transcription and repair *via* catalysis of the relaxation and unwinding of double-stranded DNA [1–7]. Recent studies showed that mammalian topoisomerase II is an important target for many anticancer agents [8–10]. Topoisomerase II inhibitors can be classified into two classes, the traditional topoisomerase II inhibitors which are called topo II poisons that act through stabilization of the formed covalent complex between the enzyme and DNA, accumulation of these complexes finally induces apoptosis [11,12]. Topo II poisons include, epipodophyllotoxin (e.g. etoposide) that binds to ATP binding site [13] and anthracyclines (e.g. doxorubicin) which bind to DNA binding site [14,15]. The recent class of topoisomerase II inhibitors are called the catalytic inhibitors (e.g. staurosporine and merbarone) [16–19] that block the catalytic activity of topo II through several mechanisms such as inhibition of topoisomerase II-mediated DNA cleavage (merbarone) [12] (Fig. 1). Nalidixic acid which is the parent of the quinolone antibiotics class showed moderate selective anticancer activity against leukemia by inhibiting topoisomerase II. However, it was reported that eukaryotic topoisomerase II less sensitive than prokaryotic topoisomerase against nalidixic acid [20]. Vosaroxin; a naphthyridine analog was found to be topoisomerase II inhibitor and is now in phase III clinical trials for the treatment of acute myeloid leukemia (AML) [21]. Ever since, many trials were made to synthesize cytotoxic agents from ciprofloxacin [22], lomefloxacin [23], norfloxacin [24] and ofloxacin [25]. Most studies were focused on the C7 piperazine ring [26–28] while little research was dedicated to the C3 carboxylic acid group. Based on the above-mentioned findings, we herein reported the design and synthesis of nalidixic acid derivatives as inhibitors of topoisomerase II enzyme *via* introduction of various moieties in position 3 such as different arylidene, pyrrole, pyrrolidine, isoindoline, arylureido and thioureido groups. At the same time, we kept the two coplanar carbonyl groups to ensure coordination with Mg^{2+} ion of topoisomerase enzyme that represents an important component of the catalytic machinery of the enzyme [29] (Fig. 2). The newly synthesized compounds were evaluated for their in vitro cytotoxic activity utilizing 60 different cancer

* Corresponding author at: Pharmaceutical Organic Chemistry, Faculty of Pharmacy, Cairo University, 33 Kasr El-Aini Street, Cairo 11562, Egypt.
E-mail address: ehab.gedawy@pharma.cu.edu.eg (E.M. Gedawy).

https://doi.org/10.1016/j.bioorg.2018.10.058
Received 28 April 2018; Received in revised form 22 October 2018; Accepted 29 October 2018
Available online 30 October 2018
0045-2068/ © 2018 Elsevier Inc. All rights reserved.

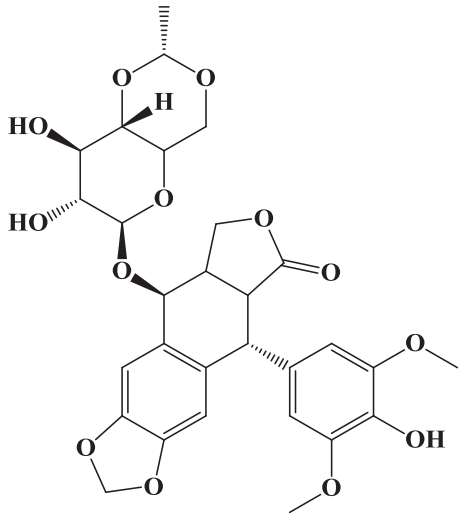

Etoposide
Inhibits topoisomerase by binding to the ATP binding site

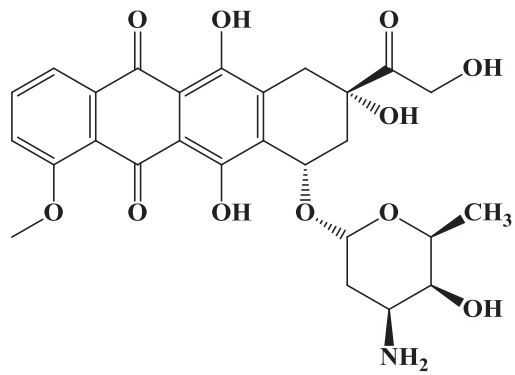

Doxorubicin
Inhibits topoisomerase by binding to the DNA binding site

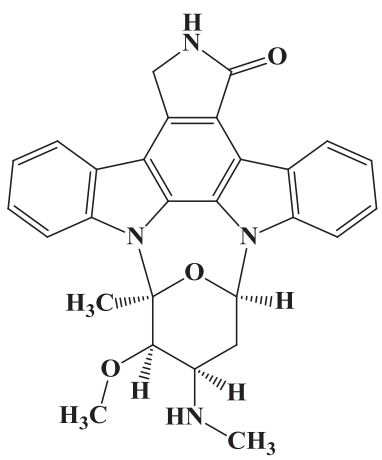

Staurosporine
Topoisomerase II catalytic inhibitor

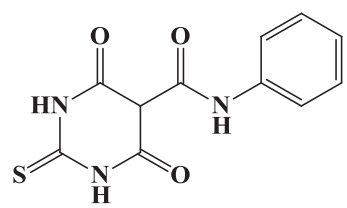

Merbarone
Topoisomerase II catalytic inhibitor (IC_{50} = 20 μM) apoptosis inducer in human leukemic CEM cells through a caspase-3-like protease-dependent mechanism.

Fig. 1. Known inhibitors for topoisomerase II.

cell lines. Also, the topoisomerase II inhibitory activity was evaluated using human DNA topoisomerase II Elisa Kit. Finally, molecular docking studies were done to predict the possible mechanism of action and binding mode for the most potent compound in order to explain its anticancer activity.

2. Results and discussion:

2.1. Chemistry

An outline for the synthesis of the target compounds is shown in Schemes 1–3. Nalidixic acid hydrazide **2** was prepared by direct hydrazinolysis of nalidixic acid **1**. Condensation of hydrazide **2** with the appropriate ketones afforded compounds **3a,b** and **4a-d**. ^{1}H NMR spectra of **3a,b** and **4a-d** revealed disappearance of NH_2 of compound **2** and appearance of only one NH signal at δ 12.44–13.19 ppm. Moreover ^{1}H NMR spectra of compounds **4a-d** disclosed appearance of the additional CH aliphatic protons of the corresponding cycloalkyl moieties. Compounds **5a-c** were prepared by reaction of the nalidixic acid hydrazide with acids anhydrides in glacial acetic acid. ^{1}H NMR spectrum of compound **5b** showed appearance of absorption band at 7.20 ppm corresponding to the two olefinic CH protons.

Reaction of compound **2** with isocyanates and isothiocyantes in absolute ethanol yielded compounds **6a,b** and **7a-d** respectively. ^{1}H NMR spectra of compounds **6a-d** revealed appearance of 3NH at 9-77-12.31 ppm while compounds **7a,b** showed 3NH at 8.54–11.28 ppm.

2.2. Biological evaluation

2.2.1. In vitro anticancer screening

All synthesized compounds were selected by the National Cancer Institute (NCI), Bethesda, USA for cytotoxic screening against 60 human cancer cell lines representing 9 tumor types including leukemia, melanoma, lung, colon, CNS, ovarian, renal, prostate, and breast cancers. Screening was performed utilizing a single dose (10^{-5} M concentration) and cell were incubated for 48 h. sulforhodamine B (SRB) dye was used for determination of end point. Results were reported as a graph representing growth percent. The percent inhibition was calculated, and the results were summarized in (Table 1). Compound **6a** showed selective potent activity against leukemia subpanal especially against k-562 and SR cell lines with growth inhibition percent of 81.11 and 57.8 respectively.

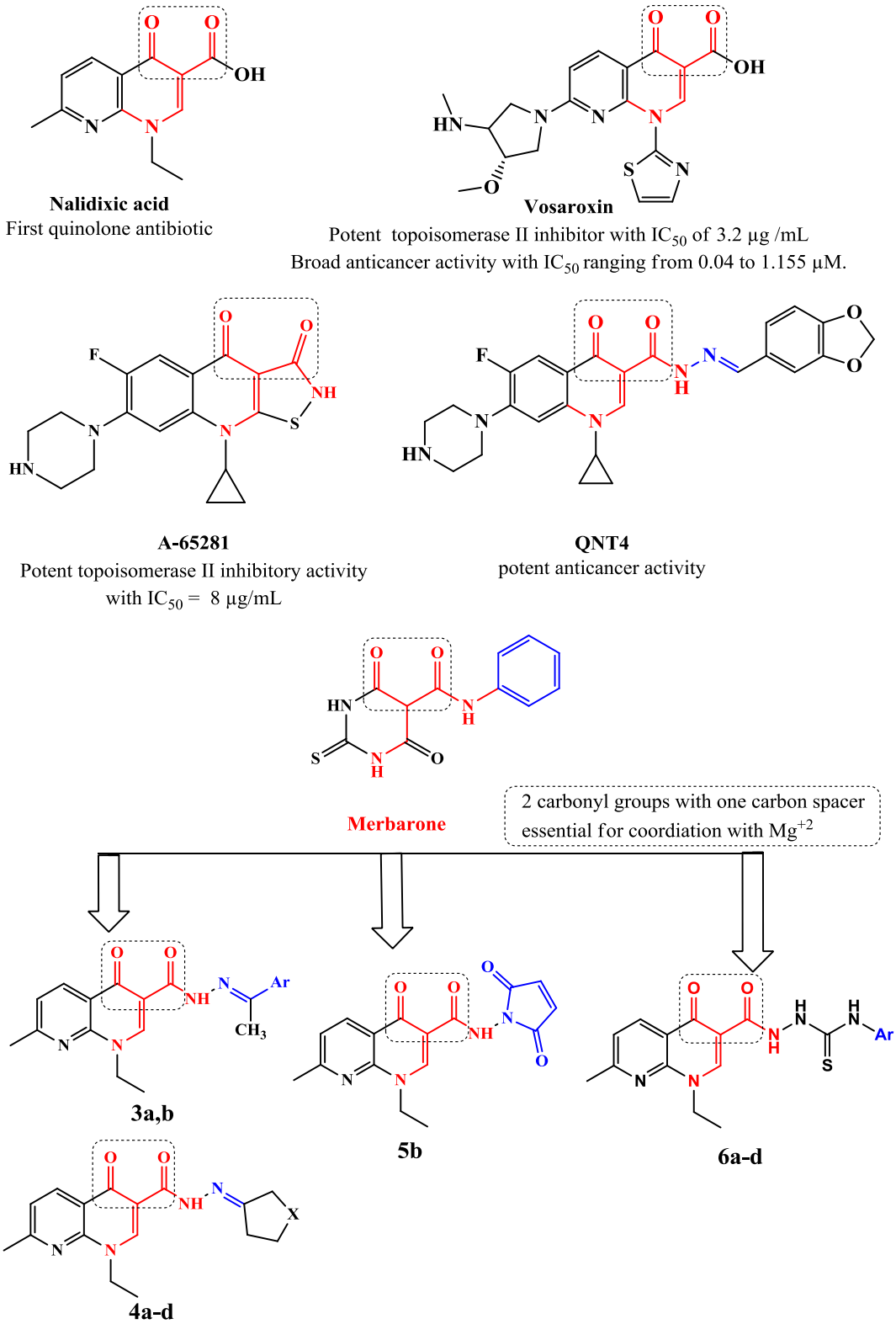

Fig. 2. Design of target compounds.

Structure activity relationship of the newly synthesized nalidixic acid derivatives disclosed that:

- Condensation of the 3-hydrazide group with aryl or cyclic aliphatic ketones (compounds **3a,b** and **4a-d**) reduced the anticancer activity. Compound **4c** showed moderate potency against K-562 and MOLT-4 Leukemia cell lines with GI% = 27.99 and 28.99, respectively. In addition, A498 renal cell line showed significant sensitivity towards compound **4c** with GI% = 42.04.
- Presence of bulky cyclic amide moiety substituted in position-3 of 1,8-naphthyridine ring (compounds **5a-c**) abolished the anticancer activity this may be attributed to the steric hindrance.

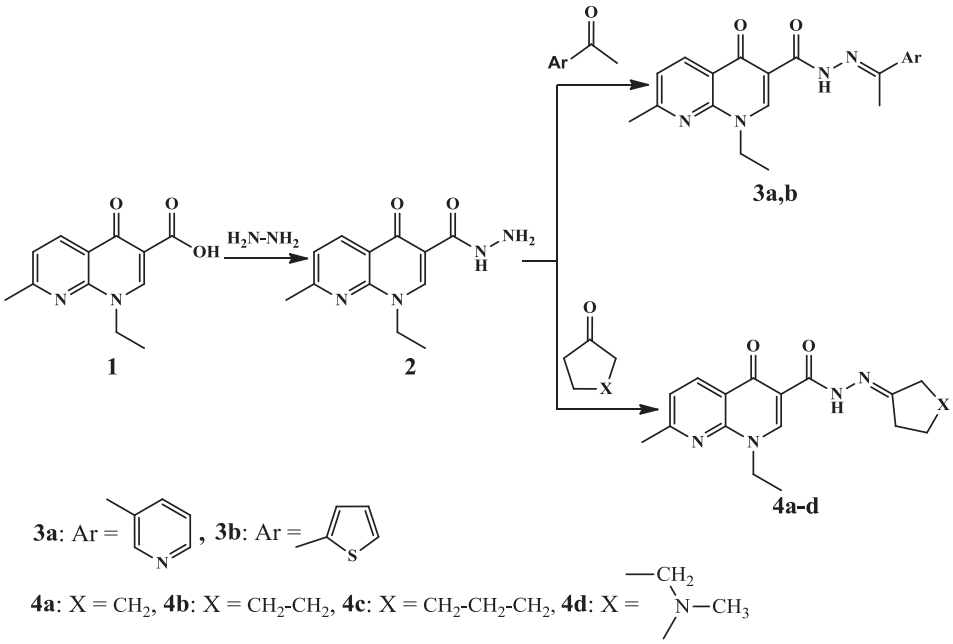

Scheme 1. Synthesis of compounds **3a,b** and **4a-d**.

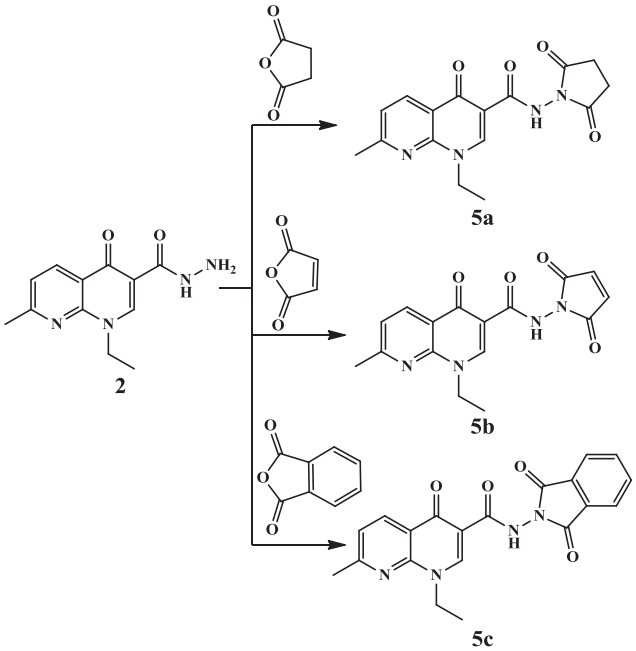

Scheme 2. Synthesis of compounds 5a-c.

- 1,8-naphthyridine-3-carbonylhydrazinecarbothioamide (thioureido derivatives, compounds **6a-d**) and 1,8-naphthyridine-3-carbonylhydrazinecarboxamide (ureido derivatives, compounds **7a,b**) showed moderate to weak anticancer activity. Concerning the substitution position on the aryl ring, meta substitution interestingly increases the potency (compound **6a** revealed potent anticancer activity against leukemia, colon, non-small cell lung and renal cancer with GI% range from 81.11 to 18.35). on the other hand, ortho and para substitution dramatically decreased the potency.

2.2.2. *In vitro cytotoxicity IC_{50} determination by MTT colorimetric assay*

Since compound **6a** showed the highest potency in the single dose in vitro screening assay, it was subjected to further studies. Five concentrations were employed for IC_{50} determination against k-562 and SR leukemia cell lines. MTT colorimetric assay was used, which determines the effect of the newly synthesized compound on the overall growth of adherent cell lines. The mitochondrial enzyme succinate dehydrogenase causes the cleavage of MTT tetrazolium salt into formazan which is a blue colored product [30]. Doxorubicin and staurosporine were used as standards. IC_{50} values, which are the concentrations required to reduce the cell growth by 50% were determined and compared to the IC_{50} achieved by doxorubicin and staurosporine. Results were demonstrated in (Fig. 3) which revealed that compound **6a** showed comparable activity with staurosporine against K-562 cell line (with IC_{50} 35.29 and 28.74 μM respectively). Moreover, **6a** was found to be equipotent with doxorubicin against SR cell lines (with IC_{50} of 13.85 and 13.83 μM respectively) additionally, it was 1.2 folds more potent than staurosporine.

2.2.3. *Cell cycle analysis*

Significant alternations in the cell phases were observed when leukemia SR cells were treated with compound 6a (Fig. 4). Results showed a decrease in the percentage of cells at the G0-G1 and S phases with 22.61% and 33.83%, respectively in comparison with control SR leukemia cell line which showed 38.31% and 55.44%, respectively. Such decrease in the percentage of cells at the G0-G1 and S phases were found to be comparable to that induced by doxorubicin (25.18% and 28.76%). On the other hand, the percentage of cells at G2-M was 43.56% which was significantly higher than control 5.25% and comparable to that of doxorubicin (46.56%). Finally, the percentage of cells at pre-G1 phase increased by 5.25 folds the control while doxorubicin caused an increase by 8.62 folds. Therefore, it can be assumed that compound **6a** exhibited cell cycle arrest at G2-M phase leading to inhibition of cell proliferation and induced apoptosis.

2.2.4. *Determination of apoptosis using annexin-V*

The results showed a significant elevation in the percentage of the early and late apoptosis when leukemia SR cells were treated with compound **6a** (3.49 and 10.92 folds, respectively more than control leukemia SR cells). Furthermore, doxorubicin revealed an increase in both the early and late apoptosis with 5.76 and 18.22 folds higher than control, respectively. Also, the necrosis percent induced by compound **6a** and doxorubicin was 2.69% and 4.08%, respectively which were noticeably higher than control that showed only 0.88% necrosis (Fig. 5).

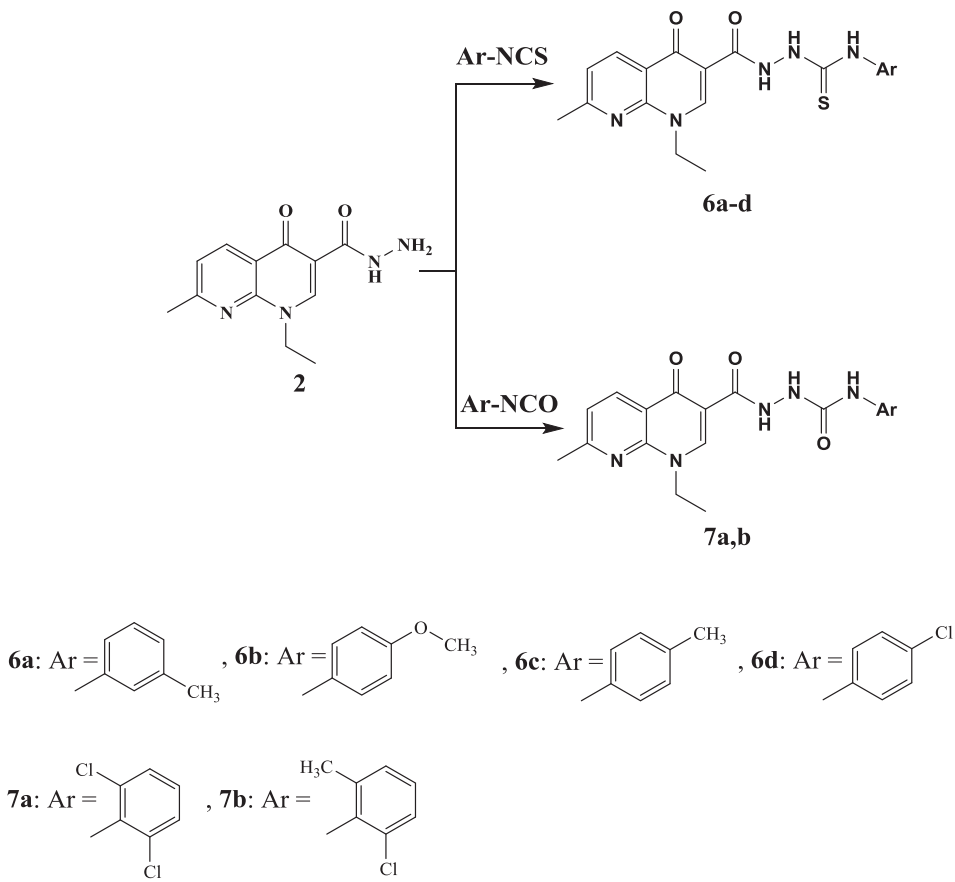

Scheme 3. Synthesis of compounds **6a-d**, **7a,b**.

2.2.5. Topoisomerase II inhibitory activity

The inhibitory activity of topoisomerase IIα and topoisomerase IIβ was evaluated for compound **6a** by using Topoisomerase Elisa Kit. Five concentrations were used and IC_{50} was calculated. Doxorubicin and topotecan, known inhibitors of topoisomerase enzymes, were used as reference. The results are reported in (Fig. 6)**.** Compound **6a** showed potent inhibitory activity against both topoisomerase II subclasses, alpha and beta with IC_{50} of 1.30 and 0.017 μM respectively which are comparable to the used standards doxorubicin and topotecan.

2.2.6. Molecular modeling study

Several crystal structures for topoisomerase enzyme were available in the protein data bank. In this work we selected (PDB ID: 4FM9) [3] which has topoisomerase IIα co-crystallized with DNA. DNA chains were removed from the active site. Molecular docking setup was validated by carrying out the docking of the inhibitor merbarone in the DNA binding site and was compared to a previously reported study [31]. The binding mode of merbarone indicated the used setup was suitable for the docking study. Merbarone demonstrated energy score (S) = −20.72 kcal/mol and was able to reproduce the coordinate bond interactions with Mg^{2+} and arene cation interaction with His 759. Compound **6a** was able to interact in a similar pattern by forming coordinate bond interactions with Mg^{2+} *via* the oxygen atoms of both carbonyl groups at positions 3 and 4, arene cation interaction with His 759 and an additional hydrogen bond with Asp 545. Compound **6a** yielded energy score (S) = −33.75 kcal/mol (Fig. 7)**.**

Concerning compounds **3a&b** and **4a-d** the steric hindrance caused by the cyclic or disubstituted hydrazones prohibited the docking poses from establishing the key interactions accomplished by the ligand, merbarone within the active site. Furthermore, the energy scores of these compounds were found to be less than that of compound **6a** (Table 6**,** Fig. 8**a,b)**. The cyclic amide structure of compounds **5a-c** seems to prevent the proper binding to the active site (Fig. 8**c)**. Compounds **6b-d** and **7a&b** yielded less energy scores (with range from −24.3206 to −30.4713 kcal/mol) than the most active compound **6a** (−33.6344). This may be due to the position of the aryl ring substituents. The meta substituent seems to fit in the active site more properly than the ortho and para positioned substituents (Fig. 8**d,e)**. The above findings could explain the low activity associated with compounds **3a&b**, **4a-d**, **5a-c**, **6b-d** and **7a&b** compared with the potent derivative **6a**.

3. Conclusion

A group of new C-3 nalidixic acid derivatives were synthesized and characterized by their spectral data. Single dose cytotoxic NCI 60 cell line screening revealed that compound **6a** has selective cytotoxic activity against leukemia especially K-562 and SR cell lines. Five dose MTT assay showed that compound **6a** has comparable anticancer activity to doxorubicin against K-562 leukemia cell line with IC_{50} 35.29 μM and it was worth mentioning that **6a** was equipotent to doxorubicin against SR leukemia cell line. Compound **6a** induced cell cycle arrest at G2-M phase that was demonstrated through accumulation of SR leukemia cells at G2-M and pre-G1 phases with increase of 8.29 and 5.28 folds respectively, relative to the control. Moreover, compound **6a** showed significant increase in the percentage of total apoptotic cells (5.28 folds more than control) and in the necrosis percentage by three folds than control. At the same time, compound **6a** also showed potent topoisomerase IIα and topoisomerase IIβ inhibitory activity with IC_{50} 1.30 and 0.017 μM respectively. Based on the molecular docking study the potent activity of **6a** can be attributed to the coordinate bonding interaction with Mg^{2+}, the hydrogen bonding with Asp 545 and the arene cation interaction with His 759. Finally, this study showed that compound **6a** represents a promising lead

Table 1
Percent inhibition for synthesized compounds at 10^{-5} Molar concentration.

Percent inhibition for synthesized compounds at 10^{-5} Molar concentration															
Cell line	**3a**	**3b**	**4a**	**4b**	**4c**	**4d**	**5a**	**5b**	**5c**	**6a**	**6b**	**6c**	**6d**	**7a**	**7b**
Leukemia															
CCRF-CEM	8.44	1.72	10.26	5.57	8.28	−0.67	4.45	7.83	7.69	50.68	15.34	9.3	3.25	8.31	3.92
HL-60(TB)	6.63	−10.16	1.2	−0.84	19.8	−2.52	6.35	1.56	−2.54	24.19	−0.96	5.5	18.36	17.05	−6.74
K-562	2.84	5.78	6.87	12.85	27.99	12.35	0.07	5.67	8.69	81.11	5.35	0.95	17.22	2.73	0.98
MOLT-4	10.97	5.88	−0.06	−3.65	28.99	2.87	0.25	0.93	−5.3	39.99	3.21	−2.31	15.16	−0.34	6.05
RPMI-8226	10.71	7.75	7.34	2.52	11.86	−1.71	−2.93	−5.36	−5.61	26.8	2.24	1.08	−4.64	5.33	−0.69
SR	9.02	6.5	0.79	−3.26	14.18	−0.12	−6.44	1.32	−10.8	57.8	10.96	−3.56	1.8	9.3	1.6
Non-Small Cell Lung Cancer															
A549/ATCC	11.52	11.92	9.68	7.8	17.41	7.68	0.91	6.19	3.98	29.6	6.91	8.36	6.99	11.95	9.21
EKVX	−2.98	2.21	11.17	1.12	6.79	−3.38	−2.46	−4.74	−8.08	32.65	5.29	−0.76	−4.41	−1.86	−6.54
HOP-62	14.33	3.39	6.7	0.46	5.23	3.41	−3.39	−0.08	−8.68	40.94	6.17	−7.93	1.65	9.4	10.99
HOP-92	12.08	6.87	9.36	13.11	19.31	4.94	−1.6	−1.09	6.05	37.62	17.26	4.91	5.44	3.77	18.85
NCI-H226	8.48	11.73	17.14	10.59	18.02	4.78	1.64	−1.62	−6.9	28.39	13.23	9.94	5.2	6.93	3.26
NCI-H23	1.29	−0.69	1.06	6.07	10.51	−0.13	−4.22	−7.15	3.46	18.98	3.15	−1.86	−1.5	−6.38	3.03
NCI-H322M	13.16	9.53	17.61	7.1	11.34	8.51	−0.01	16.25	0.96	27.79	19.5	19.62	2.96	10.06	8.13
NCI-H460	10.78	6.19	7.12	3.71	7.6	5.06	−11.17	−4.73	0.6	44.33	3.4	−0.91	−7.2	11.02	1.27
NCI-H522	13.44	8.29	11.19	4.39	24.74	5.48	5.58	9.43	0.43	49.02	9.8	2.68	12.89	8.16	16.54
Colon Cancer															
COLO 205	−4.72	−8.11	−3.66	−16.56	2.24	−6.49	−8.25	−105	−12.76	35.38	−4.68	−15.8	−9.4	−11.63	−16.96
HCC-2998	2.66	−20.27	10.39	−4.73	0.92	−17.26	−5.61	5.07	−1.62	18.35	11.51	7.27	−0.78	0.75	−9.11
HCT-116	15.11	13.23	10.88	8.48	22.28	10.65	7.24	2.9	−2.15	44.26	2.86	6.98	−3.14	5.86	13.19
HCT-15	11.02	5.91	3.45	7.11	13.85	−1.5	−0.94	2.09	0.11	66.95	16.05	−2.91	6.4	4.95	−4.15
HT29	4.81	−0.29	3.14	−1.37	0.35	−6.63	−2.23	−0.39	−4.39	32.28	4.27	2.51	−5.49	0.29	−5.5
KM12	9.29	10.38	5.32	4.09	12.37	13.27	−2.26	−1.69	3.91	32.93	7.57	−2.7	9.31	0.17	9.24
SW-620	11.65	9.02	7.04	8.38	8.81	12.1	−1.35	0.2	1.92	34.73	11.89	0.76	6.84	7.58	7.12
CNS Cancer															
SF-268	4.55	11.55	6.63	4.75	15.99	8.99	−3.16	−0.07	−2.3	33.98	7.31	−3.36	−7.84	10.45	18.52
SF-295	14.45	7.27	7.23	5.33	22.3	3.76	−0.85	−6.81	−5	39.6	6.97	−1.66	6.57	5.83	0.34
SF-539	2.88	3.64	3.77	−0.12	0.01	−4.68	−1.37	−4.2	−6.39	12.43	0.13	−2.05	−10.93	−0.12	−2.93
SNB-19	11	5.51	3.42	6.53	11.53	1.64	−0.65	3.25	0.2	32.73	6.55	−1.56	2.82	19.86	20.82
SNB-75	12.95	11.38	13.92	13.54	23.76	21.05	−1.44	2.53	−7.18	31.58	20.73	2.68	6.23	12.39	21.35
U251	4.71	0.58	3.45	3.52	5.41	5.4	4.48	0.99	2.87	42.92	3.09	6.09	3.42	20.12	24.98
Melanoma															
LOX IMVI	2.51	−4.49	1.9	3.13	5.04	−0.01	2.27	3.87	2.51	20.06	3.22	4.92	3.88	7.2	3.73
MALME-3M	3.15	−14.32	8.18	9.65	2.87	−5.09	−3.55	3.78	1.57	15.48	−1.1	−3.36	−3.49	21.94	0
M14	−3.23	−2.36	−2.18	−3.88	−3.48	−2.15	−0.64	−9.82	−13.03	31.68	−3.09	−12.79	−11.85	−4.48	−11.76
MDA-MB-435	14.34	11.49	13.07	12.64	16.08	12.14	−10.43	−4.5	−2.49	21.77	4.27	−0.72	−9.8	0.81	1.31
SK-MEL-2	4.59	−1.87	3.52	−2.29	−4.88	−0.5	−9.92	−5.46	−5.79	18.18	1.58	−4.26	−11.63	11.04	7.72
SK-MEL-28	2.86	−0.5	9.08	7.15	6.19	6.46	−16.32	−5.19	−4.55	15.06	−0.4	−4.7	−4.01	−1.89	−5.69
SK-MEL-5	11.07	−1.01	7.18	2.26	12.89	−1.89	1.9	0.12	0.59	23.02	3.16	−1.46	−2.83	0.56	−2.15
UACC-257	9.28	7.64	9.94	6.29	12.16	7.19	5.97	9.23	5.24	25.9	6.5	5.96	4.32	16.26	6.57
UACC-62	13.79	18.26	21.4	13.06	26.77	16.17	2.4	7.83	11.66	37.25	11.29	8.7	19.94	15.05	18.47
Ovarian Cancer															
IGROV1	2.7	3.63	15.01	6.24	18.46	8.18	−8.5	3.89	−8.78	28.95	7.65	4.29	1.94	0.82	−2.12
OVCAR-3	5.01	6.61	5.74	8.77	13.75	4.2	5.17	−4.73	0.7	32.58	7.12	−2.93	2.52	−3.64	−3.6
OVCAR-4	5.99	−0.67	16.34	13.08	20.36	7.11	−3.97	−5.59	−1.05	44.58	11.03	−2.18	−1.6	3.03	−0.16
OVCAR-5	11.02	5.64	5.96	2.38	7.42	4.05	−5.27	−4.22	−8.08	30.44	6.56	−7.22	−8.26	−1.73	−8.29
OVCAR-8	6.8	3.96	10.03	2.83	7.47	0.47	−4.82	2.78	4.77	33.02	5.94	4.36	4.44	6.59	1.48
NCI/ADR-RES	6.37	0.55	10.19	3.59	10.6	−8.53	−6.15	−8.72	−4.61	38.6	4.85	4.35	−2.14	5.82	−4.07
SK-OV-3	6.34	3.18	8.82	9.39	1.82	3.21	−0.4	1.91	4.92	9.03	10.19	−5.76	0.02	1.18	9
Renal Cancer															
786-0	8.4	9.91	6.94	9.36	12.77	3.57	−6.97	−4.21	−3.18	19.76	7.33	−2.49	−5.63	8.64	1.5
A498	11.38	17.82	33.25	22.45	42.04	19.43	11.86	21.53	16.29	50.6	25.39	23.59	18.89	0.52	20.4
ACHN	7.79	3.26	13.41	8.82	15.32	0.05	−12.43	−2.43	1.7	36.94	6.5	4.52	1.35	1.99	1.16
CAKI-1	15.29	8.32	15.8	12.42	20.1	18.04	6.31	7.96	1.19	44.28	16.47	4.56	2.56	3.4	11.76
RXF 393	−7.98	−0.9	−3.04	−5.66	−0.14	2.38	−10.26	−1.67	−3.87	22.51	11.02	−3.83	−13.38	−3.37	8.16
SN12C	22.62	17.74	18.95	14.85	14.53	16	−1.49	5.16	13.66	22.99	8.99	11.43	9.19	19.15	13.68
TK-10	−6.43	−8.49	0.04	−4.75	4.33	−6.35	−5.14	−8.18	−1.71	26.63	−3.26	−0.17	0.56	7.07	−0.93
UO-31	17.1	12.8	18.69	14.74	24.84	10.45	11.77	14.73	13.05	46.07	24.44	21.14	18.55	12.35	4.71
Prostate Cancer															
PC-3	12.02	8.94	14.36	11.22	17.31	12.27	8.05	7.04	6.94	42.04	10.43	9.78	16.07	10.37	8.14
DU-145	−0.65	−0.1	−9.32	−10.81	10.79	−2.13	−8.17	−9.11	−5.17	25.62	−4.38	−7.82	7.13	−0.68	−2
Breast Cancer															
MCF7	20.06	12.39	16.61	10.83	22.84	10.09	8.18	6.74	5.62	45.93	16.64	2.76	7.88	11.23	7.15
MDA-MB-231/ATCC	12.34	16.82	6.68	5.61	12.86	−4.52	−5.63	−4.16	0.53	38.09	3.05	6.48	0.68	20.69	16.3
HS 578T	16.35	23.93	11.18	18.13	19.88	17.24	0.54	−2.67	8.74	53.54	7.37	4.15	10.59	22.25	26.45
BT-549	3.34	2.09	16.54	8.05	17.03	2.89	−2.09	−2.32	−4.95	27.26	7.22	2.93	−0.01	7.21	5.93
T-47D	11.94	16.29	11.02	7.66	22.8	9.79	6.95	4.8	3.93	36.38	6.95	11.93	13.16	8.48	3.98
MDA-MB-468	−0.74	21.89	8.24	13.1	14.11	5.65	1.64	−11.88	−4.42	30.98	8.79	12.02	−11.92	−3.4	16.09

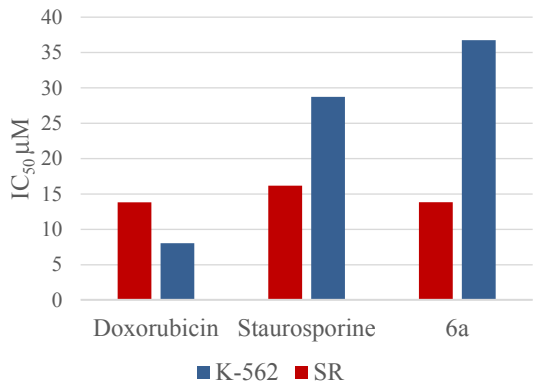

Fig. 3. Bar presentation graph showing IC_{50} against K-562 and SR cell lines for compound **6a**.

topoisomerase II inhibitor and a selective cytotoxic agent against leukemia that requires further investigation.

4. Experimental

4.1. Chemistry

Chemicals were purchased from Sigma-Aldrich, USA and Acros Organics, Belgium. The reactions progress was monitored by TLC using precoated aluminum sheet silica gel MERCK 60F 254 (Merck, Germany) and was visualized by UV lamp. The solvent system used was chloroform: benzene: methanol [9:5:1]. Melting points were obtained using Stuart electrothermal melting point apparatus SMP10 and were uncorrected. ^{1}H NMR spectra were carried out using a Bruker Advance 400 MHz NMR spectrometer. ^{13}C NMR spectra were carried out using a Bruker Advance 100 MHz spectrometer. Chemical shifts were recorded in ppm on δ scale using DMSO-d_6 as solvent and coupling constants (*J*) in Hz. Mass spectra were run at 70 ev on Hewlett Packard 5988 spectrometer, Micro Analytical Center, Cairo University, Egypt. Element analyses were carried out at the Regional Center for Mycology and Biotechnology, Faculty of Pharmacy, Al Azhar University, Egypt.

4.1.1. Synthesis of 1-ethyl-7-methyl-4-oxo-1,4-dihydro-1,8-naphthyridine-3-carbohydrazide (Nalidixic acid hydrazide) (2)

A mixture of nalidixic acid **1** (0.01 mol, 2.31 g) and hydrazine hydrate (100%, 25 mL) was heated under reflux for 24 h. The reaction mixture was allowed to cool. The formed precipitate was filtered, dried and recrystallized from 70% ethanol to afford **2**; mp: 192–193 °C (as reported) [32]; Yield: 1.67 g, 68%.

4.1.2. General procedure for the synthesis of 1-ethyl-7-methyl-4-oxo-N'-(1-(aryl)ethylidene)-1,4-dihydro-1,8-naphthyridine-3-carbohydrazide (3a,b).

Nalidixic acid hydrazide **2** (0.25 g, 1 mmol) was dissolved in 10 mL absolute ethanol containing 0.20 mL glacial acetic acid. Equimolar amount of the heterocyclic ketone was added and the solution was heated under reflux for 6 h. The formed precipitate was filtered while hot and recrystallized from methanol to afford **3a,b**.

4.1.2.1. 1-Ethyl-7-methyl-4-oxo-N'-(1-(pyridin-3-yl)ethylidene)-1,4-dihydro-1,8-naphthyridine-3-carbohydrazide (3a).

Creamy white solid; mp: > 300 °C; yield: 0.32 g, 91.40%; IR (KBr) νmax: 3421 (NH), 1678 (C=O) cm^{-1}; ^{1}H NMR (400 MHz, DMSO-d_6): δ 1.44 (t, 3H, CH_3, J = 7.0 Hz), 2.44 (s, 3H, CH_3), 2.71 (s, 3H, CH_3), 4.66–4.68 (q, 2H, CH_2, J = 7.0 Hz), 7.49 (t, 1H, ArH, J = 8.0 Hz), 7.56 (d, 1H, ArH, J = 8.0 Hz), 8.23 (d, 1H, ArH, J = 8.0 Hz), 8.62–8.64 (m, 1H, ArH), 8.67 (d, 1H, ArH, J = 8.0 Hz), 9.03 (s, 1H, ArH), 9.17 (s, 1H, ArH) and 13.19 (s, 1H, NH, D_2O exchangeable) ppm; MS [*m/z*, %]: 350 [M + 1]$^{\cdot+}$, 2.27], 349 [M$^+$, 2.46] and 215 [M - $C_7H_8N_3$]$^{\cdot+}$, 100]; Anal. Calcd for $C_{19}H_{19}N_5O_2$ (349.39): C, 65.32; H, 5.48; N, 20.04. Found: C, 65.49; H, 5.70; N, 20.31.

4.1.2.2. 1-Ethyl-7-methyl-4-oxo-N'-(1-(thiophen-2-yl)ethylidene)-1,4-dihydro-1,8-naphthyridine-3-carbohydrazide (3b).

Buff solid; mp: > 300 °C; yield: 0.30 g, 83.30%; IR (KBr) νmax: 3340 (NH), 1670 (C=O) cm^{-1}; ^{1}H NMR (400 MHz, DMSO-d_6): δ 1.43 (t, 3H, CH_3, J = 7.0 Hz), 2.43 (s, 3H, CH_3), 2.70 (s, 3H, CH_3), 4.63–4.68 (q, 2H, CH_2, J = 7.0 Hz), 7.11–7.13 (m, 1H, ArH), 7.54–7.56 (m, 2H, ArH), 7.62 (d, 1H, ArH, J = 8.0 Hz), 8.65 (d, 1H, ArH, J = 8.0 Hz), 9.13 (s, 1H, ArH) and 13.05 (s, 1H, NH, D_2O exchangeable) ppm; ^{13}C NMR (100 MHz, DMSO-d_6): δ 14.79, 15.53, 25.34, 46.86, 112.07, 119.83, 122.22, 127.97, 128.33, 129.08, 136.44, 143.53, 147.00, 148.46, 148.74, 160.57, 163.96 and 176.51; MS [*m/z*, %]: 355 [M + 1]$^{\cdot+}$, 13.37], 354 [M$^{\cdot+}$, 53.87] and 215 [M - $C_6H_7N_2S$]$^{\cdot+}$, 100]; Anal. Calcd for $C_{18}H_{18}N_4O_2S$ (354.43): C, 61.00; H, 5.12; N, 15.81. Found: C, 60.78; H, 5.24; N, 15.97.

4.1.3. General procedure for the synthesis of compounds 4a-d.

To a solution of nalidixic acid hydrazide **2** (0.25 g, 1 mmol) in 25 mL hot distilled water the appropriate cyclic ketone (1 mmol) was added, then the mixture was stirred vigorously for 24 h. The formed precipitate was filtered and recrystallized from absolute ethanol to yield compounds **4a-d**.

4.1.3.1. N1-Cyclopentylidene-1-ethyl-7-methyl-4-oxo-1,4-dihydro-1,8-naphthyridine-3-carbohydrazide (4a).

Buff solid; mp: 238–240 °C; yield: 0.19 g, 59.40%; IR (KBr) νmax: 3143 (NH), 1670 (C=O) cm^{-1}; ^{1}H NMR (400 MHz, DMSO-d_6): δ 1.41 (t, 3H, CH_3, J = 7.0 Hz), 1.74–1.79 (m, 2H, CH_2), 1.84–1.88 (m, 2H, CH_2), 2.35–2.43 (m, 4H, $2CH_2$), 2.68 (s, 3H, CH_3), 4.58–4.63 (q, 2H, CH_2, J = 7.0 Hz), 7.50 (d, 1H, ArH, J = 8.2 Hz), 8.58 (d, 1H, ArH, J = 8.2 Hz), 9.09 (s, 1H, ArH) and 12.44 (s, 1H, NH, D_2O exchangeable) ppm; ^{13}C NMR (100 MHz, DMSO-d_6): δ 15.47, 24.73, 24.98, 25.33, 28.83, 33.00, 46.75, 112.03, 119.79, 122.18, 136.44, 148.44, 148.75, 160.30, 163.93, 166.63 and 176.3 ppm; MS [*m/z*, %]: 313 [M + 1]$^{\cdot+}$, 24.2], 312 [M$^{\cdot+}$, 100] and 215 [M - $C_5H_9N_2$]$^{\cdot+}$, 95.47]; Anal. Calcd for $C_{17}H_{20}N_4O_2$ (312.37): C, 65.37; H, 6.45; N, 17.94. Found: C, 65.51; H, 6.53; N, 18.12.

4.1.3.2. N1-Cyclohexylidene-1-ethyl-7-methyl-4-oxo-1,4-dihydro-1,8-naphthyridine-3-carbohydrazide (4b).

Buff solid; mp: 252–254 °C; yield: 0.24 g, 72.70%; IR (KBr) νmax: 3136 (NH), 1670 (C=O) cm^{-1}; ^{1}H NMR (400 MHz, DMSO-d_6): δ 1.41 (t, 3H, CH_3, J = 7.0 Hz), 1.63–1.68 (m, 6H, $3CH_2$), 2.32–2.35 (m, 2H, CH_2), 2.45–2.48 (m, 2H, CH_2), 2.67 (s, 3H, CH_3), 4.59–4.64 (q, 2H, CH_2, J = 7.0 Hz), 7.49 (d, 1H, ArH, J = 8 Hz), 8.57 (d, 1H, ArH, J = 8 Hz), 9.08 (s, 1H, ArH) and 12.79 (s, 1H, NH, D_2O exchangeable) ppm; ^{13}C NMR (100 MHz, DMSO-d_6): δ 15.52, 25.35, 25.56, 26.02, 27.18, 27.60, 35.20, 46.72, 112.32, 119.83, 122.17, 136.48, 148.48, 148.76, 159.55, 160.60, 163.92 and 176.40 ppm; MS [*m/z*, %]: 327 [M + 1]$^{\cdot+}$, 26.1] and 326 [M$^+$, 100]; Anal. Calcd for $C_{18}H_{22}N_4O_2$ (326.39): C, 66.24; H, 6.79; N, 17.17. Found: C, 65.98; H, 6.87; N, 17.41.

4.1.3.3. N^1-Cycloheptylidene-1-ethyl-7-methyl-4-oxo-1,4-dihydro-1,8-naphthyridine-3-carbohydrazide (4c).

Buff solid; mp: 255–257 °C; yield: 0.26 g, 74.10%; IR (KBr) νmax: 3132 (NH), 1685 (C=O) cm^{-1}; ^{1}H NMR (400 MHz, DMSO-d_6): δ 1.41 (t, 3H, CH_3, J = 7.0 Hz), 1.58–1.62 (m, 6H, $3CH_2$), 1.76–1.79 (m, 2H, CH_2), 2.48–2.50 (m, 4H, $2CH_2$), 2.69 (s, 3H, CH_3), 4.59–4.65 (q, 2H, CH_2, J = 7.0 Hz), 7.51 (d, 1H, ArH, J = 8.2 Hz), 8.60 (d, 1H, ArH, J = 8.2 Hz), 9.10 (s, 1H, ArH) and 12.63 (s, 1H, NH, D_2O exchangeable) ppm; ^{13}C NMR (100 MHz, DMSO-d_6): δ 15.48, 24.34, 25.32, 27.59, 30.12, 30.19, 31.26, 36.77, 46.00, 112.16, 119.77, 122.16, 136.48, 148.42, 148.73, 158.23, 162.07, 163.94 and 171.68 ppm; MS [*m/z*, %]: 341 [M + 1]$^{\cdot+}$, 22.24], 340 [M$^+$, 81.0] and 215 [M - $C_7H_{13}N_2$]$^{\cdot+}$, 100]; Anal. Calcd for $C_{19}H_{24}N_4O_2$ (340.42): C, 67.04; H, 7.11; N, 16.46. Found: C, 67.23; H, 7.04; N, 16.59.

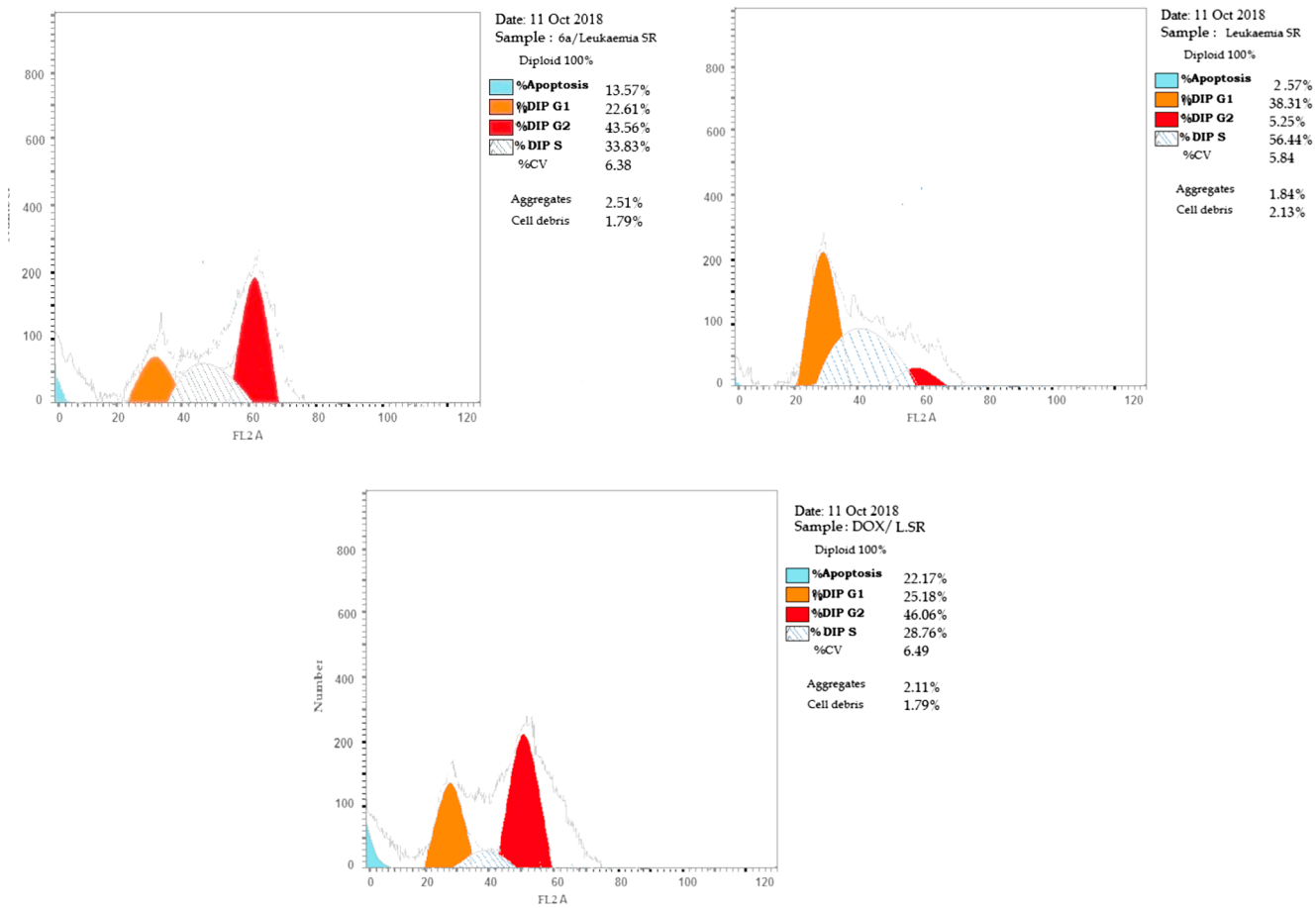

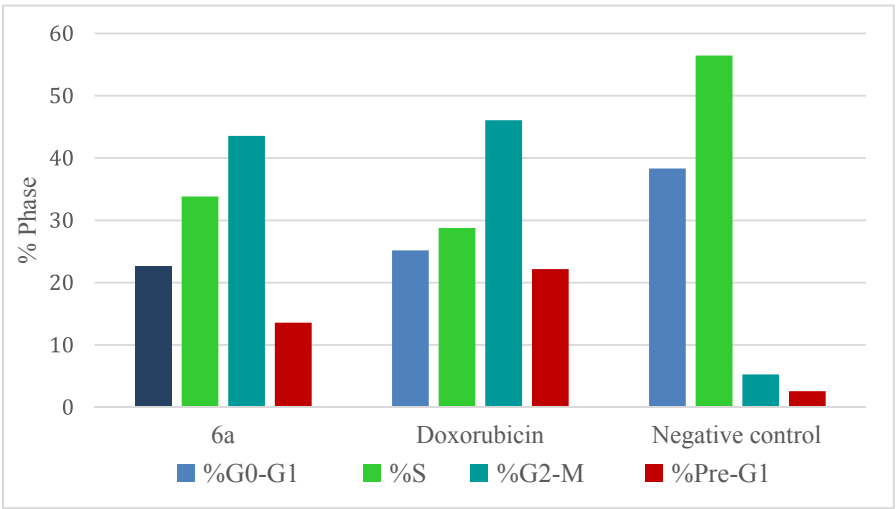

Fig. 4. Effect of compound **6a** on DNA-ploidy flow cytometric analysis of leukemia SR cells in comparison with doxorubicin and negative control.

4.1.3.4. 1-Ethyl-7-methyl-N[1]-(1-methylpiperidin-4-ylidene)-4-oxo-1,4-dihydro-1,8-naphthyridine-3-carbohydrazide (4d). Buff solid; mp: 238–240 °C; yield: 0.27 g, 79.40%; IR (KBr) νmax: 3132 (NH), 1685 (C=O) cm^{-1}; ^1H NMR (400 MHz, DMSO-d_6): δ 1.41 (t, 3H, CH_3, J = 7.0 Hz), 2.25 (s, 3H, CH_3), 2.43–2.45 (m, 2H, CH_2), 2.52–2.54 (m, 2H, CH_2), 2.67 (s, 3H, CH_3), 3.35–3.50 (m, 4H, $2CH_2$), 4.58–4.63 (q, 2H, CH_2, J = 7.0 Hz), 7.48 (d, 1H, ArH, J = 8.2 Hz), 8.56 (d, 1H, ArH, J = 8.2 Hz), 9.08 (s, 1H, ArH) and 12.81 (s, 1H, NH, D_2O exchangeable) ppm; ^{13}C NMR (100 MHz, DMSO-d_6): δ 15.48, 25.34, 27.54, 34.35, 45.77, 46.77, 54.33, 55.84, 112.12, 119.76, 122.21, 136.42, 148.43, 148.73, 156.38, 160.69, 163.98 and 176.37 ppm; MS [m/z, %]: 342 [M $+1^{\cdot+}$, 0.64], 341 [M^+, 1.55] and 110 [$C_6H_{10}N_2^{\cdot+}$, 100] Anal. Calcd for $C_{18}H_{23}N_5O_2$ (341.41): C, 63.32; H, 6.79; N, 20.51. Found: C, 63.50; H, 6.86; N, 20.74.

4.1.4. General procedure for the synthesis of compounds 5a-c.

Equimolar amounts of Nalidixic acid hydrazide **2** (0.25 g, 1 mmol) and the selected acid anhydride were dissolved in glacial acetic acid and heated under reflux for 12 h. The reaction mixture was allowed to cool, filtered, dried and recrystallized from absolute ethanol to give compounds **5a-c.**

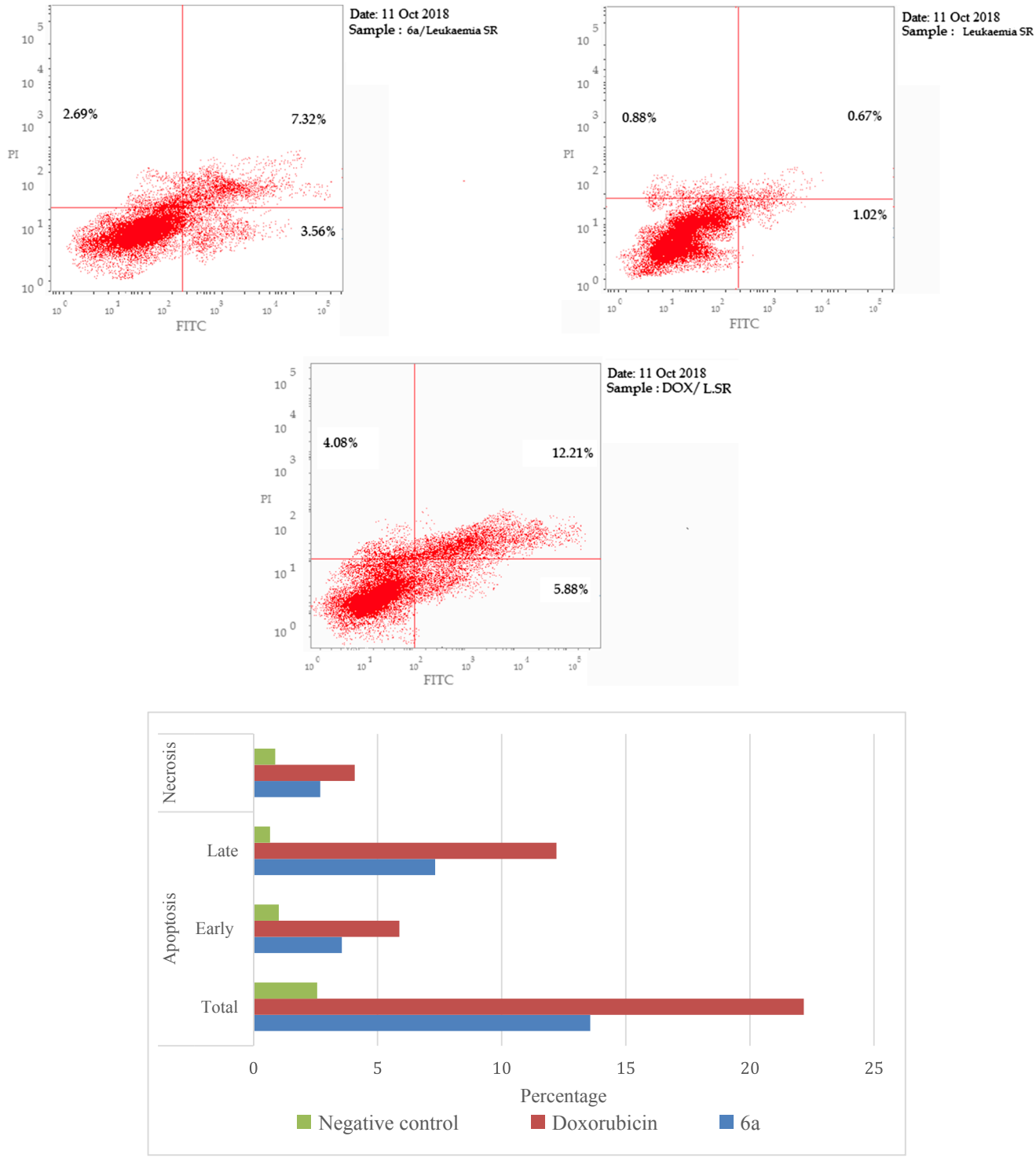

Fig. 5. Effect of compound **6a** on the percentage of Annexin-V-FITC-positive staining in leukemia SR cells in comparison with doxorubicin and negative control.

4.1.4.1. N-(2,5-Dioxopyrrolidin-1-yl)-1-ethyl-7-methyl-4-oxo-1,4-dihydro-1,8-naphthyridine-3-carboxamide (5a). Buff solid; mp: 260–262 °C; yield: 0.27 g, 81%; IR (KBr) νmax: 3278 (NH), 1732 (C=O), 1670 (C=O) cm^{-1}; ^{1}H NMR (400 MHz, DMSO-d_6): δ 1.41 (t, 3H, CH_3, J = 7.0 Hz), 1.80 (s, 4H, $2CH_2$), 2.69 (s, 3H, CH_3), 4.60–4.62 (q, 2H, CH_2, J = 7.0 Hz), 7.52 (d, 1H, ArH, J = 8.0 Hz), 8.59 (d, 1H, ArH, J = 8.0 Hz), 9.02 (s, 1H, ArH) and 11.60 (s, 1H, NH, D_2O exchangeable) ppm; ^{13}C NMR (400 MHz, DMSO-d_6): δ 15.45, 20.83, 25.34, 26.84, 46.80, 110.58, 111.42, 120.01, 122.39, 136.41, 148.49, 149.37, 161.69, 163.42, 166.82 and 175.85 ppm; MS [m/z, %]: 329 [M $+1]^{\cdot+}$, 2.61], 328 [$M^{\cdot+}$, 12.35] and 215 [M - $C_4H_5N_2O_2]^{\cdot+}$, 100]; Anal. Calcd for $C_{16}H_{16}N_4O_4$ (328.32): C, 58.53; H, 4.91; N, 17.06. Found: C, 58.67; H, 5.08; N, 17.23.

4.1.4.2. N-(2,5-Dioxo-2,5-dihydro-1H-pyrrol-1-yl)-1-ethyl-7-methyl-4-oxo-1,4-dihydro-1,8-naphthyridine-3-carboxamide (5b). Pale yellow solid; mp: 265–267 °C; yield: 0.24 g, 72%; IR (KBr) νmax: 3510 (NH), 1732 (C=O), 1670 (C=O) cm^{-1}; ^{1}H NMR (400 MHz, DMSO-d_6): δ 1.41 (t, 3H, CH_3, J = 7.0 Hz), 2.69 (s, 3H, CH_3), 4.57–4.62 (q, 2H, CH_2, J = 7.0 Hz), 7.20 (s, 2H, 2CH), 7.53 (d, 1H, ArH, J = 8.1 Hz), 8.59 (d,

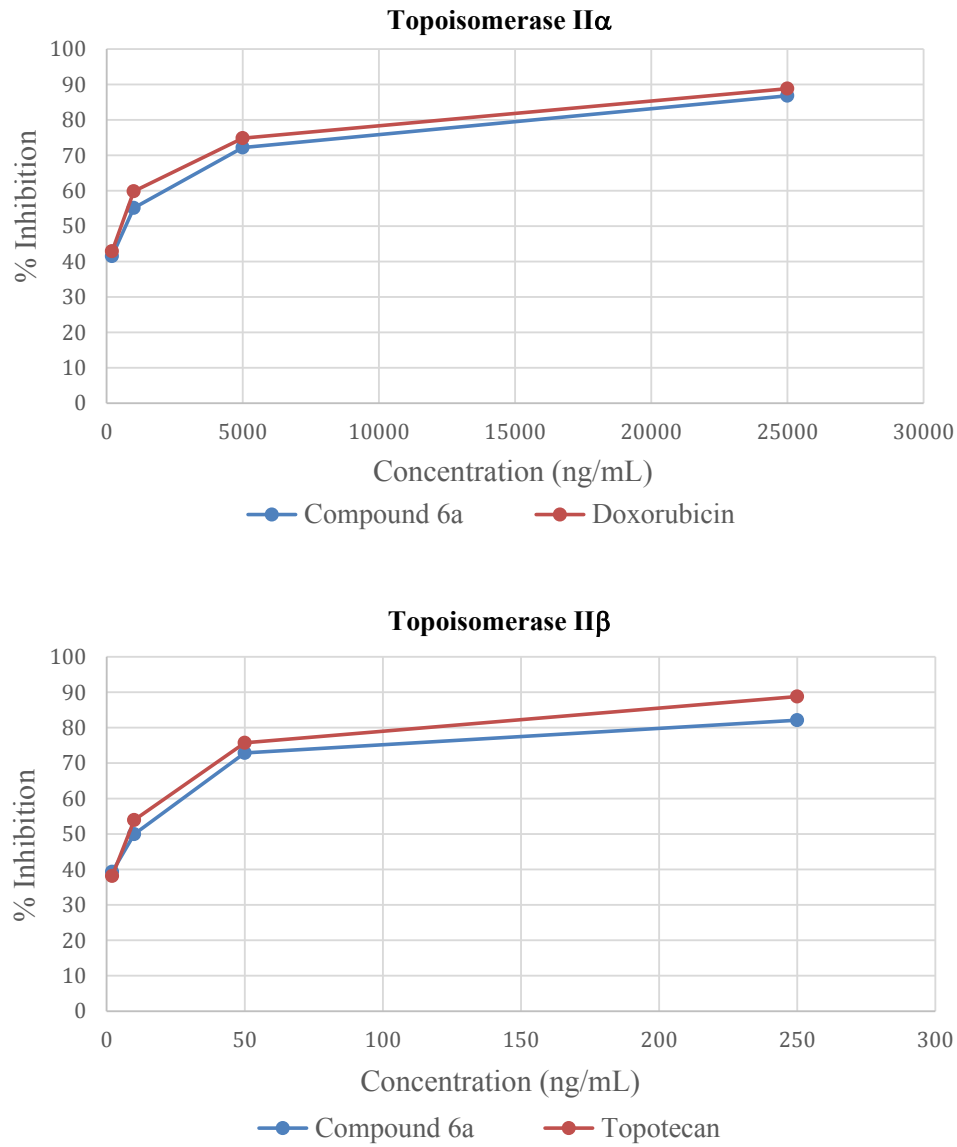

Fig. 6. Dose response curve presentation showing IC_{50} against Topoisomerase IIα and Topoisomerase IIβ for compound **6a**.

1H, ArH, $J = 8.1$ Hz), 9.03 (s, 1H, ArH) and 11.35 (s, 1H, NH, D_2O exchangeable) ppm; ^{13}C NMR (100 MHz, DMSO-d_6): δ 15.43, 25.35, 46.80, 110.43, 120.11, 122.40, 134.20, 136.47, 148.65, 149.56, 164.05, 164.27, 168.41 and 175.94 ppm; MS [*m/z*, %]: 327 [M + 1]$^{+}$, 4.66], 326 [M^{+}, 22.14] and 215 [M - $C_4H_3N_2O_2$]$^{+}$, 100]; Anal. Calcd for $C_{16}H_{14}N_4O_4$ (326.31): C, 58.89; H, 4.32; N, 17.17. Found: C, 59.12; H, 4.23; N, 17.03.

4.1.4.3. N-(1,3-Dioxoisoindolin-2-yl)-1-ethyl-7-methyl-4-oxo-1,4-dihydro-1,8-naphthyridine-3-carboxamide (5c). Pale yellow solid; mp: 298–298 °C; yield: 0.35 g, 92%; IR (KBr) νmax: 3522 (NH), 1747 (C=O) cm^{-1}; ^{1}H NMR (400 MHz, DMSO-d_6): δ 1.42 (t, 3H, CH_3, $J = 7.0$ Hz), 2.70 (s, 3H, CH_3), 4.58–4.63 (q, 2H, CH_2, $J = 7.0$ Hz), 7.54 (d, 1H, ArH, $J = 8.0$ Hz), 7.94–8.00 (m, 4H, ArH), 8.60 (d, 1H, ArH, $J = 8.0$ Hz), 9.07 (s, 1H, ArH) and 11.60 (s, 1H, NH, D_2O exchangeable) ppm; ^{13}C NMR (100 MHz, DMSO-d_6): δ 15.45, 25.36, 46.84, 110.46, 120.12, 122.43, 124.13, 130.16, 135.61, 136.46, 148.65, 149.59, 164.10, 164.23, 165.55 and 176.02 ppm; MS [*m/z*, %]: 377 [M + 1]$^{+}$, 25.56], 376 [M^{+}, 100] and 215 [M - $C_8H_5N_2O_2$]$^{+}$, 100]; Anal. Calcd for $C_{20}H_{16}N_4O_4$ (376.37): C, 63.82; H, 4.28; N, 14.89. Found: C, 63.70; H, 4.41; N, 14.95.

4.1.5. General procedure for the synthesis of compounds 6a-d.

1-Ethyl-7-methyl-4-oxo-1,4-dihydro-1,8-naphthyridine-3-carbohydrazide (**2**) (0.50 g, 2 mmol) and the appropriate isothiocyanate (2 mmol) were dissolved in absolute ethanol and heated under reflux for 5 h. The reaction mixture was left to cool and the formed precipitate was filtered, dried and recrystallized from 95% ethanol to yield compounds **6a-d**.

4.1.5.1. 2-(1-Ethyl-7-methyl-4-oxo-1,4-dihydro-1,8-naphthyridine-3-carbonyl)-N-(m-tolyl)hydrazinecarbothioamide (6a). White solid; mp: > 300 °C; yield: 0.70 g, 87.50%; IR (KBr) νmax: 3286 (NH), 1643 (C=O) cm^{-1}; ^{1}H NMR (400 MHz, DMSO-d_6): δ 1.41 (t, 3H, CH_3, $J = 7.0$ Hz), 2.29 (s, 3H, CH_3), 2.69 (s, 3H, CH_3), 4.59–4.64 (q, 2H, CH_2, $J = 7.0$ Hz), 6.95 (d, 1H, ArH, $J = 7.6$ Hz), 7.2 (t, 1H, ArH, $J = 7.6$ Hz), 7.31–7.36 (m, 2H, ArH), 7.52 (d, 1H, ArH, $J = 8.0$ Hz), 8.60 (d, 1H, ArH, $J = 8.0$ Hz), 9.05 (s, 1H, ArH), 9.79 (s, 2H, 2NH, D_2O exchangeable) and 10.53 (s, 1H, NH, D_2O exchangeable) ppm; ^{13}C NMR (100 MHz, DMSO-d_6): δ 15.54, 21.46, 25.36, 46.62, 111.72, 119.98, 122.20, 125.59, 125.78, 128.48, 128.61, 136.51, 137.95, 138.10, 139.59, 148.47, 148.56, 152.07, 163.89 and 175.83 ppm; MS [*m/z*, %]: 396 [M + 1]$^{+}$, 2.46], 395 [M^{+}, 9.19] and 91 [C_7H_7]$^{+}$, 100]; Anal. Calcd for $C_{20}H_{21}N_5O_2S$ (395.48): C, 60.74; H, 5.35; N, 17.71. Found: C, 60.51; H, 5.44; N, 17.92.

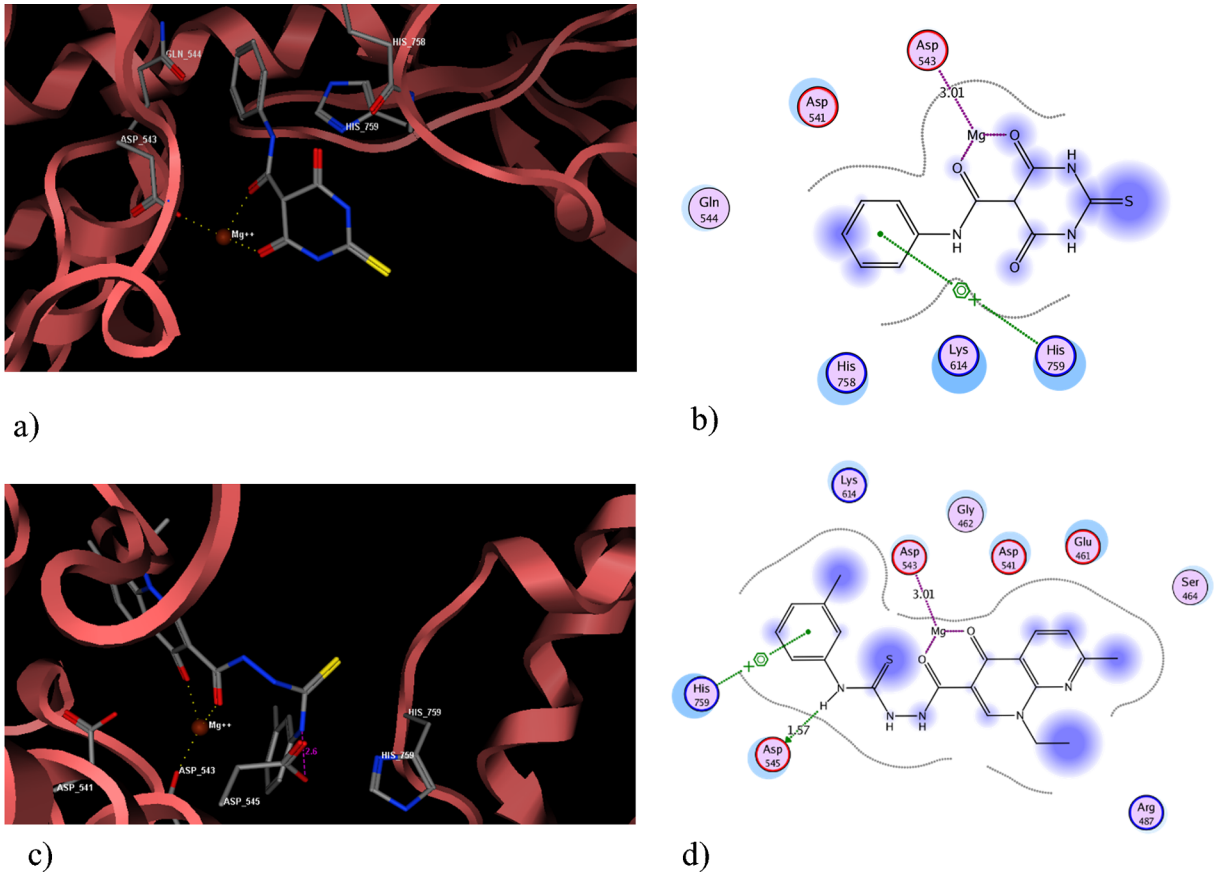

Fig. 7. (a) 3D interaction of merbarone with DNA binding site of topoisomerase IIα, (b) 2D interaction of merbarone with DNA binding site of topoisomerase IIα, (c) 3D interaction of compound **6a** with DNA binding site of topoisomerase IIα and (d) 2D interaction of **6a** with DNA binding site of topoisomerase IIα.

4.1.5.2. 2-(1-Ethyl-7-methyl-4-oxo-1,4-dihydro-1,8-naphthyridine-3-carbonyl)-N-(4-methoxyphenyl)hydrazinecarbothioamide (6b). White solid; mp: 276–278 °C; yield: 0.76 g, 92.40%; IR (KBr) νmax: 3286 (NH), 1651 (C=O) cm^{-1}; ^{1}H NMR (400 MHz, DMSO-d_6): δ 1.41 (t, 3H, CH_3, J = 7.0 Hz), 2.69 (s, 3H, CH_3), 3.75 (s, 3H, CH_3), 4.59–4.65 (q, 2H, CH_2, J = 7.0 Hz), 6.89 (d, 2H, 2ArH, J = 8.8 Hz), 7.35 (d, 2H, 2ArH, J = 6.8 Hz), 7.52 (d, 1H, ArH, J = 8.0 Hz), 8.61 (d, 1H, ArH, J = 8.0 Hz), 9.05 (s, 1H, ArH), 10.07 (s, 1H, NH, D_2O exchangeable), 11.44 (s, 1H, NH, D_2O exchangeable) and 12.23 (s, 1H, NH, D_2O exchangeable) ppm; ^{13}C NMR (100 MHz, DMSO-d_6): δ 15.33, 25.23, 46.90, 55.64, 110.33, 113.96, 119.75, 122.36, 127.68, 131.93, 136.31, 144.34, 148.33, 157.25, 162.03, 164.29, 171.26 and 175.95 ppm; MS [m/z, %]: 412 [M + 1]$^{+}$, 0.46], 411 [M^{+}, 1.68] and 215 [M - $C_8H_{10}N_3OS$]$^{+}$, 100]; Anal. Calcd for $C_{20}H_{21}N_5O_3S$ (411.48): C, 58.38; H, 5.14; N, 17.02. Found: C, 58.38; H, 5.27; N, 16.89.

4.1.5.3. 2-(1-Ethyl-7-methyl-4-oxo-1,4-dihydro-1,8-naphthyridine-3-carbonyl)-N-(p-tolyl)hydrazinecarbothioamide (6c). White solid; mp: 250–252 °C; yield: 0.64 g, 81%; IR (KBr) νmax: 3286 (NH), 1651 (C=O) cm^{-1}; ^{1}H NMR (400 MHz, DMSO-d_6): δ 1.41 (t, 3H, CH_3, J = 7.0 Hz), 2.28 (s, 3H, CH_3), 2.69 (s, 3H, CH_3), 4.59–4.64 (q, 2H, CH_2, J = 7.0 Hz), 7.13 (d, 2H, 2ArH, J = 8.0 Hz), 7.34–7.38 (m, 2H, 2ArH), 7.51 (d, 1H, ArH, J = 8.0 Hz), 8.60 (d, 1H, ArH, J = 8.0 Hz), 9.04 (s, 1H, ArH), 9.77 (s, 1H, NH, D_2O exchangeable), 10.38 (s, 1H, NH, D_2O exchangeable) and 12.31 (s, 1H, NH, D_2O exchangeable) ppm; ^{13}C NMR (100 MHz, DMSO-d_6): δ 15.26, 20.85, 25.18, 46.86, 111.17, 119.56, 122.29, 125.07, 129.26, 133.50, 135.06, 136.10, 136.46, 148.14, 152.20, 164.16, 169.24 and 175.76 ppm; MS [m/z, %]: 396 [M + 1]$^{+}$, 2.46], 395 [M^{+}, 2.12] and 215 [M - $C_8H_{10}N_3S$]$^{+}$, 100]; Anal. Calcd for $C_{20}H_{21}N_5O_2S$ (395.48): C, 60.74; H, 5.35; N, 17.71. Found: C, 60.89; H, 5.52; N, 17.54.

4.1.5.4. N-(4-Chlorophenyl)-2-(1-ethyl-7-methyl-4-oxo-1,4-dihydro-1,8-naphthyridine-3-carbonyl)hydrazinecarbothioamide (6d). White solid; mp: 293–295 °C; yield: 0.70 g, 84%; IR (KBr) νmax: 3286 (NH), 1651 (C=O) cm^{-1}; ^{1}H NMR (400 MHz, DMSO-d_6): δ 1.41 (t, 3H, CH_3, J = 7.0 Hz), 2.69 (s, 3H, CH_3), 4.59–4.64 (q, 2H, CH_2, J = 7.0 Hz), 7.38 (d, 2H, 2ArH, J = 8.8 Hz), 7.52 (d, 1H, ArH, J = 8.0 Hz), 7.55–7.58 (m, 2H, 2ArH), 8.60 (d, 1H, ArH, J = 8.0 Hz), 9.05 (s, 1H, ArH), 9.91 (s, 1H, NH, D_2O exchangeable), 10.70 (s, 1H, NH, D_2O exchangeable) and 11.33 (s, 1H, NH, D_2O exchangeable) ppm; ^{13}C NMR (100 MHz, DMSO-d_6): δ 15.34, 25.24, 46.88, 115.86, 119.74, 122.32, 128.60, 128.96, 136.28, 138.19, 148.31, 164.23, 173.63 and 175.88 ppm; MS [m/z, %]: 416 [M + 1]$^{+}$, 0.09], 415 [M^{+}, 0.31] and 215 [M - $C_7H_7ClN_3S$]$^{+}$, 100]; Anal. Calcd for $C_{19}H_{18}ClN_5O_2S$ (415.90): C, 54.87; H, 4.36; N, 16.84. Found: C, 54.95; H, 4.08; N, 16.95.

4.1.6. General procedure for the synthesis of compounds 7a,b.

A mixture of Nalidixic acid hydrazide **2** (0.25 g, 1 mmol) and the appropriate aryl isocyanate (1 mmol) in absolute ethanol was heated under reflux for 5 h. The reaction mixture was left to cool and the formed precipitate was filtered, dried and recrystallized from 95% ethanol to afford white solid (**7a.b**).

4.1.6.1. N-(2,6-Dichlorophenyl)-2-(1-ethyl-7-methyl-4-oxo-1,4-dihydro-1,8-naphthyridine-3-carbonyl)hydrazinecarboxamide (7a). White solid; mp: 308–310 °C; yield: 0.28 g, 64.50%; IR (KBr) νmax: 3294 (NH), 1693 (C=O), 1643 (C=O) cm^{-1}; ^{1}H NMR (400 MHz, DMSO-d_6): δ 1.41 (t, 3H, CH_3, J = 7.0 Hz), 2.69 (s, 3H, CH_3), 4.61 (q, 2H, CH_2, J = 7.0 Hz), 7.30 (t, 1H, ArH, J = 8 Hz), 7.50–7.53 (m, 3H, ArH), 8.54 (s, 1H, NH, D_2O exchangeable), 8.60 (d, 1H, ArH, J = 8.0 Hz), 8.81 (s, 1H, NH, D_2O exchangeable), 9.08 (s, 1H, ArH) and 11.28 (s, 1H, NH, D_2O exchangeable) ppm; ^{13}C NMR (100 MHz, DMSO-d_6): δ 15.45, 25.31,

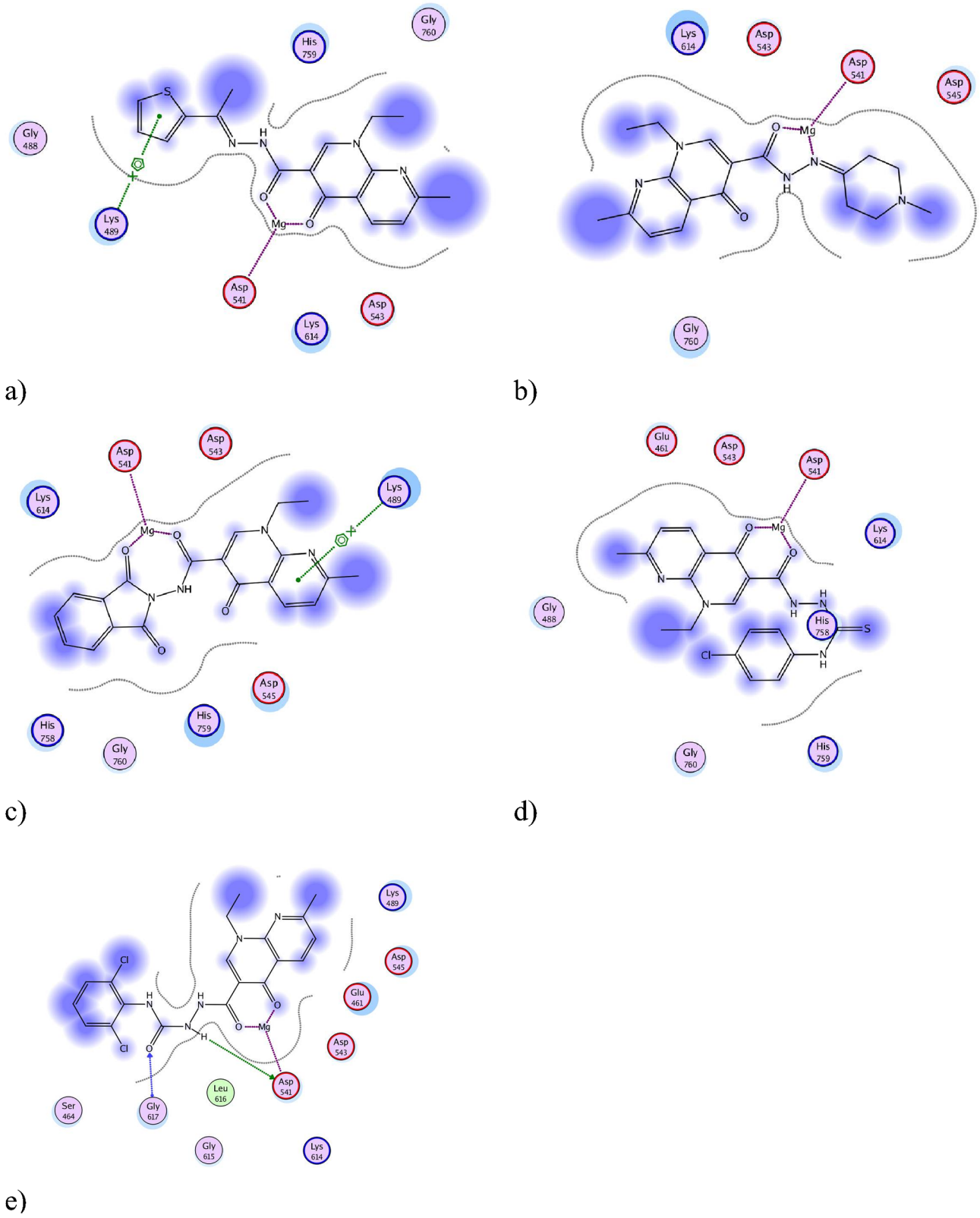

Fig. 8. (a) 2D interaction of compound **3b** with DNA binding site of topoisomerase IIα, (b) 2D interaction of compound **4d** with DNA binding site of topoisomerase IIα, (c) 2D interaction of compound **5c** with DNA binding site of topoisomerase IIαα, (d) 2D interaction of compound **6d** with DNA binding site of topoisomerase IIα, (e) 2D interaction of compound **7a** with DNA binding site of topoisomerase IIα.

46.54, 111.92, 117.47, 118.62, 119.86, 121.96, 128.47, 128.88, 128.98, 136.38, 141.52, 147.81, 148.43, 148.53, 163.75, 163.84 and 175.89 ppm; MS [*m/z*, %]: 435 [M+1]$^{+}$, 0.23], 434 [M^{+}, 0.09] and 215 [M - $C_7H_6Cl_2N_3O$]$^{+}$, 100]; Anal. Calcd for $C_{19}H_{17}Cl_2N_5O_3$ (434.28): C, 52.55; H, 3.95; N, 16.13. Found: C, 52.78; H, 4.07; N, 16.40.

4.1.6.2. N-(2-Chloro-6-methylphenyl)-2-(1-ethyl-7-methyl-4-oxo-1,4-dihydro-1,8-naphthyridine-3-carbonyl)hydrazinecarboxamide (7b). White

solid; mp: 308–310 °C; yield: 0.29 g, 65.90%; IR (KBr) νmax: 3309 (NH), 1697 (C=O), 1651 (C=O) cm^{-1} ^{1}H NMR (400 MHz, DMSO-d_6): δ 1.41 (t, 3H, CH_3, J = 7.0 Hz), 2.25 (s, 3H, CH_3), 2.69 (s, 3H, CH_3), 4.59–4.64 (q, 2H, CH_2, J = 7.0 Hz), 7.15–7.22 (m, 2H, ArH), 7.32 (d, 1H, ArH, J = 6.5 Hz), 7.51 (d, 1H, ArH, J = 8.0 Hz), 8.29 (s, 1H, NH, D_2O exchangeable), 8.60 (d, 1H, ArH, J = 8.0 Hz), 8.65 (s, 1H, NH, D_2O exchangeable), 9.07 (s, 1H, ArH) and 11.23 (s, 1H, NH, D_2O exchangeable) ppm; ^{13}C NMR (100 MHz, DMSO-d_6): δ 15.52, 18.88, 25.34, 49.06, 120.19, 122.20, 123.88, 127.22, 127.79, 129.43, 132.53, 134.35, 136.51, 143.60, 148.57, 151.20, 153.41, 163.64, 163.92 and 176.01 ppm; MS [m/z, %]: 414 [M + 1]$^{+}$, 0.27], 413 [M^{+}, 0.96] and 215 [M - $C_8H_9ClN_3O$]$^{+}$, 100]; Anal. Calcd for $C_{20}H_{20}ClN_5O_3$ (434.28): C, 58.04; H, 4.87; N, 16.92. Found: C, 58.21; H, 5.11; N, 16.78.

4.2. Biological evaluation

4.2.1. In vitro anticancer screening

60 different human cancer cell lines were utilized to screen the newly synthesized compounds for anticancer activity according to the previously reported standard procedure [33–35] as follows:

1. RPMI 160 medium containing 2 mM L-glutamine and fetal bovine serum was used to grow the human cancer cell lines.
2. Cells were inoculated into 96 well microtiter plates into 100 µL at optical density ranging from 4000 to 5000 cells/well depending on the replication time of individual cell lines.
3. The microtiter plates were incubated at 37 °C, 5% CO_2, 95% air and 100% relative humidity for 24 h.
4. Trichloroacetic acid (TCA) was used to fix two plates of each cell line *in situ*. This represented a measurement of cell population at the time of drug addition (Tz).
5. The synthesized compounds were dissolved in dimethyl sulfoxide (DMSO) at 400 folds the desired final maximum concentration and frozen prior to use.
6. The frozen concentrate was melted at time of drug addition and diluted to twice the final concentration with complete medium containing 50 µg/mL gentamycin.
7. 100 µL of the synthesized compounds were added to the appropriate microtiter wells already containing 100 µL yielding the final compound concentration.
8. Following the compounds addition, the plates were incubated at 37 °C, 5% CO_2, 95% air and 100% relative humidity for 48 h.
9. 50 µL of cold 50% (w/v) TCA was gently added to fix the cells and the plates were incubated for 60 min at 4 °C. The supernatant was discarded and the plates are washed 5 times with tap water and air dried.
10. To each well, sulphorhodamine B (SRB) solution (100 µL) at 0.4% (w/v) in 1% acetic acid was added and plates were incubated for 10 min at room temperature.
11. Unbound dye was removed by washing five times with 1% acetic acid and plates were air dried.
12. 10 mµ trizma base was used to dissolve the bound stain and the absorbance was read at 415 nm wavelength using an automated plate reader.
13. The percentage growth inhibition was calculated as:

$$\left[\frac{(Ti - Tz)}{C - Tz}\right] \times 100 \quad for \quad concentrations \quad which \quad Ti \geq Tz$$

$$\left[\frac{(Ti - Tz)}{Tz}\right] \times 100 \quad for \quad concentrations \quad which \quad Ti < Tz$$

Where Time zero is Tz, Control growth is C, Test growth in the presence of drug is Ti.

4.2.2. MTT colorimetric assay

Determination of IC_{50} using MTT colorimetric assay was done according to the previously reported standard procedure [36–41] as follows:

1. Leukemia K-562 and SR cells were obtained from the American Type Culture Collection. K-562 and SR cells were grown in 100 µL DMEM media in a U-bottomed 96-well microtiter tray, supplemented with 50 µg/mL penicillin and 25 µg/mL streptomycin and were incubated at 37 °C till the concentration of the suspended cells in the media was 5 × 10^4 cells/mL.
2. The tested compound and standards were dissolved in DMEM media at 1 mg/mL concentration. 10 folds serial dilutions were made directly in the 96 well microtiter tray to obtain the final desired concentrations (100, 10, 1, 0.1, 0.01 µg/mL) and were incubated for 24 h at 37 °C.
3. MTT (3-(4,5-dimethylthiazol-2-yl)-2,5-diphenyltetrazolium bromide was dissolved in in phosphate buffered saline at concentration 5 mg/mL. 10 µL of MTT solution was added to all wells in the microtiter plate. Incubate the cultures at 37 °C for 2 h.
4. 100 µL of isopropanol acidified with HCl (2 mL concentrated HCl added to 500 mL isopropanol) were added to each well to dissolve the formed formazan crystals. Gentle agitation was applied to ensure complete dissolution of the formazan crystals.
5. The absorbance was measured spectrophotometrically at two different wavelengths (540 nm and 690 nm) and the results were summarized in **(**Table 2**).**

4.2.3. Cell cycle analysis

The effect of compound **6a** on cell cycle progression was analyzed by flow cytometric analysis according to the following procedure [42]:

1. Leukemia SR cells were treated with compound **6a** at concentration of IC_{50} (13.85 uM) and incubated for 24 h.
2. Ice-cold phosphate buffer saline (PBS) was used to wash the cells twice.
3. Cells were collected by centrifugation, fixed in 70% (v/v) ethanol, washed with PBS and re-suspended with 0.1 mg/mL RNase.
4. Cells then were stained with 40 mg/mL propidium iodide (PI) and evaluated by flow cytometry using FACSCalibur (Becton Dickinson).
5. Cell Quest software (Becton Dickinson) was used to calculate cell cycle distributions and the results were summarized in **(**Table 3**).**

4.2.4. Determination of apoptosis using Annexin-V

Evaluation of the pro-apoptotic effect of compound **6a** was done using Annexin-V-FITC and propidium iodide using the following procedure[42]:

1. Leukemia SR cells were incubated for 24 h after treatment with compound **6a** at its IC_{50} (13.85 µM).
2. The cells were then collected by trypsinization and 0.5 × 10^6 cells were washed twice with PBS and stained with 5 mL Annexin-V-FITC and 5 mL PI in 1 × binding buffer for 15 min at room temperature in the dark.
3. Analysis were performed using FACS Calibur flow cytometer (BD Biosciences, San Jose, CA) and the results were reported in **(**Table 4**).**

Table 2
IC_{50} against K-562 and SR cell lines for compound **6a**.

Compounds	IC_{50} µM Leukemia cell line	
	K-562	SR
6a	35.28	13.85
Staurosporine	28.74	16.18
Doxorubicin	8.05	13.83

Table 3
Cell cycle analysis of compound **6a,** doxorubicin and negative control for leukemia SR cells.

Cell cycle phase	%G0-G1	%S	%G2-M	%Pre-G1
6a	22.61	33.83	43.56	13.57
Doxorubicin	25.18	28.76	46.06	22.17
Negative control	38.31	56.44	5.25	2.57

Table 4
Apoptosis results of negative control and compound **6a**, doxorubicin and for leukemia SR cells.

	Apoptosis			Necrosis
	%Total	%Early	%Late	
6a	13.57	3.56	7.32	2.69
Doxorubicin	22.17	5.88	12.21	4.08
Negative control	2.57	1.02	0.67	0.88

Table 5
Topoisomeraese IIα and IIβ IC_{50} for compound **6a.**

	IC_{50} μM	
Compounds	**Topoisomerase IIα**	**Topoisomerase IIβ**
6a	1.30	0.017
Topotecan		0.014
Doxorubicin	0.98	

Table 6
Energy scores obtained from the molecular docking study.

Compound	Energy score
3a	−28.0148
3b	−29.55
4a	−29.8803
4b	−32.8026
4c	−26.8890
4d	−27.9011
5a	−28.7625
5b	−27.4704
5c	−33.8068
6a	−33.6344
6b	−24.3206
6c	−30.4713
6d	−27.8352
7a	−26.3692
7b	−27.8352

4.2.5. Topoisomerase II inhibitory activity

Compound **6a** was evaluated for topoisomerase IIα and topoisomerase IIβ inhibitory activity utilizing the human DNA topoisomerase Elisa kit and following the provided procedure:

1. Standards and the tested compound were dissolved in sample diluent and 2 folds serial dilution was achieved.
2. Biotin-conjugated antibody and avidin conjugated Horseradish Peroxidase (HRP-avidin) were diluted to 10 folds.
3. 100 μL of each concentration of standard or test compound were added to each well. Incubate at 37 °C for 1 h.
4. The liquid in each well was removed.
5. 100 μL of Biotin-conjugated antibody solution was added to each well followed by incubation for 1 h at 37 °C.
6. The microtiter plate was allowed to aspirate and washed 3 times.
7. 100 μL of avidin conjugated Horseradish Peroxidase (HRP-avidin) solution was added to each well and the plate was incubated for 1 h at 37 °C.
8. The plate was aspirated and washed 5 times.
9. 90 μL of TMB substrate were added to each well and the plate was incubated for 30 min at 37 °C and protected from light.
10. 50 μL stop solution was added. The absorbance was measured spectrophotometrically within 5 min at 450 nm and the results were summarized in (Table 5).

4.2.6. Molecular modeling study

Molecular modeling studies were carried out using Molecular Operating Environment (MOE, 10.2008) software. All minimizations were carried out with MOE with MMFF94x force field and the partial and formal charges were automatically calculated. The x-ray crystallographic structures of topoisomerase IIα co-crystallized with DNA [3] were downloaded from the protein data bank [43]. Enzyme was prepared for docking study by removal of DNA chains, water molecules. Protonate 3D protocol in MOE with default options was used to prepare the topoisomerase enzyme. For the docking protocol triangle matcher placement method and London dG scoring function were used. Validation of the docking setup was done by docking of the reference topoisomerase inhibitor merbarone and comparing the results with a previously reported study [31]. The MOE validated setup was used to predict the binding interactions and affinity of the synthesized compounds at the active site. Reference compound merbarone was used to compare its binding score and binding interactions with the nalidixic acid derivatives. Energy scores of all the synthesized compounds are shown in (Table 6).

Acknowledgment

Authors wish to express their deepest gratitude to the Development Therapeutics Program of the National Cancer Institute, Bethesda, MD, USA, for in vitro evaluation of anticancer activity. The authors are thankful Dr. Esam Rashwan, Head of the confirmatory diagnostic unit VACSERA-EGYPT, for carrying out *in vitro* topoisomerase II inhibition assays and cell cycle analysis. This work was funded by the Faculty of Pharmacy, Cairo University, Egypt.

References

[1] T.R. Strick, V. Croquette, D. Bensimon, Single-molecule analysis of DNA uncoiling by a type II topoisomerase, Nature 404 (2000) 901–904.
[2] M.R. Redinbo, L. Stewart, P. Kuhn, J.J. Champoux, W.G.J. Hol, Crystal structures of human topoisomerase I in covalent and noncovalent complexes with DNA, Science 279 (1998) 1504–1513.
[3] T.J. Wendorff, B.H. Schmidt, P. Heslop, C.A. Austin, J.M. Berger, The structure of DNA-bound human topoisomerase II alpha: conformational mechanisms for coordinating inter-subunit interactions with DNA cleavage, J. Mol. Biol. 424 (2012) 109–124.
[4] A.J. Schoeffler, J.M. Berger, Recent advances in understanding structure–function relationships in the type II topoisomerase mechanism, Biochem. Soc. Trans. 33 (2005) 1465–1470.
[5] H. Wei, A.J. Ruthenburg, S.K. Bechis, G.L. Verdine, Nucleotide-dependent domain movement in the ATPase domain of a human type IIA DNA topoisomerase, J. Biol. Chem. 280 (2005) 37041–37047.
[6] J.C. Wang, DNA topoisomerases, Annu. Rev. Biochem. 65 (1996) 635–692.
[7] J.M. Berger, Structure of DNA topoisomerases, Biochim. Biophys. Acta. 1400 (1998) 3–18.
[8] U. Kellner, P. Rudolph, R. Parwaresch, Human DNA-topoisomerases–diagnostic and therapeutic implications for cancer, Oncol. Res. Treat. 23 (2000) 424–430.
[9] A.Y. Chen, L.F. Liu, DNA topoisomerases: essential enzymes and lethal targets, Annu. Rev. Pharmacol. Toxicol. 34 (1994) 191–218.
[10] S.H. Kaufmann, Cell death induced by topoisomerase-targeted drugs: more questions than answers, Biochim. Biophys. Acta (BBA)-Gene Struct, Expr. 1400 (1998) 195–211.
[11] W.T. Beck, S.E. Morgan, Y.-Y. Mo, U.G. Bhat, Tumor cell resistance to DNA topoisomerase II inhibitors: new developments, Drug Resist. Updat. 2 (1999) 382–389.
[12] J.M. Fortune, N. Osheroff, Merbarone inhibits the catalytic activity of human topoisomerase IIα by blocking DNA cleavage, J. Biol. Chem. 273 (1998) 17643–17650.
[13] D. Leroy, A.V. Kajava, C. Frei, S.M. Gasser, Analysis of Etoposide Binding to Subdomains of Human DNA Topoisomerase II α in the Absence of DNA,

Biochemistry 40 (2001) 1624–1634.
[14] C.J. Lee, J.S. Kang, M.S. Kim, K.P. Lee, M.S. Lee, The study of doxorubicin and its complex with DNA by SERS and UV-resonance Raman spectroscopy, Bull. Korean Chem. Soc. 25 (2004) 1211–1216.
[15] A. Bodley, L.F. Liu, M. Israel, R. Seshadri, Y. Koseki, F.C. Giuliani, S. Kirschenbaum, R. Silber, M. Potmesil, DNA topoisomerase II-mediated interaction of doxorubicin and daunorubicin congeners with DNA, Cancer Res. 49 (1989) 5969–5978.
[16] P. Lassota, G. Singh, R. Kramer, Mechanism of topoisomerase II inhibition by staurosporine and other protein kinase inhibitors, J. Biol. Chem. 271 (1996) 26418–26423.
[17] N. Pastor, I. Domínguez, M.L. Orta, C. Campanella, S. Mateos, F. Cortés, The DNA topoisomerase II catalytic inhibitor merbarone is genotoxic and induces endoreduplication, Mutat. Res. Mol. Mech. Mutagen. 738 (2012) 45–51.
[18] J.J. Dimaggio, R.P. Warrell, J. Muindi, Y.W. Stevens, S.J. Lee, D.A. Lowenthal, I. Haines, T.D. Walsh, L. Baltzer, S. Yaldaei, Phase I clinical and pharmacological study of merbarone, Cancer Res. 50 (1990) 1151–1155.
[19] T. Khélifa, W.T. Beck, Merbarone, a catalytic inhibitor of DNA topoisomerase II, induces apoptosis in CEM cells through activation of ICE/CED-3-like protease, Mol. Pharmacol. 55 (1999) 548–556.
[20] Y. Yamashita, T. Ashizawa, M. Morimoto, J. Hosomi, H. Nakano, Antitumor quinolones with mammalian topoisomerase II mediated DNA cleavage activity, Cancer Res. 52 (1992) 2818–2822.
[21] A.K. Hotinski, I.D. Lewis, D.M. Ross, Vosaroxin is a novel topoisomerase-II inhibitor with efficacy in relapsed and refractory acute myeloid leukaemia, Expert Opin. Pharmacother. 16 (2015) 1395–1402.
[22] Z. Shi, Y. Li, Y. Kang, G. Hu, C. Huang-Fu, J. Deng, B. Liu, Piperonal ciprofloxacin hydrazone induces growth arrest and apoptosis of human hepatocarcinoma SMMC-7721 cells, Acta Pharmacol. Sin. 33 (2012) 271.
[23] Y. Zhou, X. Xu, Y. Sun, H. Wang, H. Sun, Q. You, Synthesis, cytotoxicity and topoisomerase II inhibitory activity of lomefloxacin derivatives, Bioorg. Med. Chem. Lett. 23 (2013) 2974–2978.
[24] K.C. Fang, Y.L. Chen, J.Y. Sheu, T.C. Wang, C.C. Tzeng, Synthesis, antibacterial, and cytotoxic evaluation of certain 7-substituted norfloxacin derivatives, J. Med. Chem. 43 (2000) 3809–3812.
[25] G. Hu, G. Wang, N. Duan, X. Wen, T. Cao, S. Xie, W. Huang, Design, synthesis and antitumor activities of fluoroquinolone C-3 heterocycles (IV): s-triazole Schiff-Mannich bases derived from ofloxacin, Acta Pharm. Sin. B. 2 (2012) 312–317.
[26] S. Rajabalian, A. Foroumadi, A. Shafiee, S. Emami, Functionalized N-(2-oxyiminoethyl) piperazinyl quinolones as new cytotoxic agents, J. Pharm. Pharm. Sci. 10 (2007) 153–158.
[27] J. Azéma, B. Guidetti, J. Dewelle, B. Le Calve, T. Mijatovic, A. Korolyov, J. Vaysse, M. Malet-Martino, R. Martino, R. Kiss, 7-((4-Substituted) piperazin-1-yl) derivatives of ciprofloxacin: synthesis and in vitro biological evaluation as potential antitumor agents, Bioorg. Med. Chem. 17 (2009) 5396–5407.
[28] A.A.M. Abdel-Aziz, A.S. El-Azab, A.M. Alanazi, Y.A. Asiri, I.A. Al-Suwaidan, A.R. Maarouf, R.R. Ayyad, T.Z. Shawer, Synthesis and potential antitumor activity of 7-(4-substituted piperazin-1-yl)-4-oxoquinolines based on ciprofloxacin and norfloxacin scaffolds: in silico studies, J. Enzyme Inhib. Med. Chem. 31 (2016) 796–809.
[29] C. Sissi, M. Palumbo, Effects of magnesium and related divalent metal ions in topoisomerase structure and function, Nucl. Acids Res. 37 (2009) 702–711.
[30] T.F. Slater, B. Sawyer, U. Sträuli, Studies on succinate-tetrazolium reductase systems: III. Points of coupling of four different tetrazolium salts III. Points of coupling of four different tetrazolium salts, Biochim. Biophys. Acta 77 (1963) 383–393.
[31] A.T. Baviskar, S.M. Amrutkar, N. Trivedi, V. Chaudhary, A. Nayak, S.K. Guchhait, U.C. Banerjee, P.V. Bharatam, C.N. Kundu, Switch in site of inhibition: a strategy for structure-based discovery of human Topoisomerase IIα catalytic inhibitors, ACS Med. Chem. Lett. 6 (2015) 481–485.
[32] F. Carroll, B.D. Berrang, C.P. Linn, Synthesis of naphthyridinone derivatives as potential antimalarials, J. Heterocycl. Chem. 18 (1981) 941–946.
[33] M.C. Alley, D.A. Scudiere, A. Monks, M.L. Hursey, M.J. Czerwinski, D.L. Fine, B.J. Abbott, J.G. Mayo, R.H. Shoemaker, M.R. Boyd, Feasibility of Drug Screening with Panels of Human Tumor Cell Lines Using a Microculture Tetrazolium Assay1, Cancer Res. 48 (1988) 589–601.
[34] M.R. Boyd, K.D. Paull, Some practical considerations and applications of the National Cancer Institute in vitro anticancer drug discovery screen, Drug Dev. Res. 34 (1995) 91–109.
[35] M.R. Grever, S.A. Schepartz, B.A. Chabner, The National Cancer Institute: cancer drug discovery and development program, Semin. Oncol. 19 (1992) 622–638.
[36] H. Takeuchi, M. Baba, S. Shigeta, An application of tetrazolium (MTT) colorimetric assay for the screening of anti-herpes simplex virus compounds, J. Virol. Methods 33 (1991) 61–71.
[37] J. Carmichael, W.G. DeGraff, A.F. Gazdar, J.D. Minna, J.B. Mitchell, Evaluation of a tetrazolium-based semiautomated colorimetric assay: assessment of chemosensitivity testing, Cancer Res. 47 (1987) 936–942.
[38] J.M. Edmondson, L.S. Armstrong, A.O. Martinez, A rapid and simple MTT-based spectrophotometric assay for determining drug sensitivity in monolayer cultures, J. Tissue Cult. Methods 11 (1988) 15–17.
[39] F. Denizot, R. Lang, Rapid colorimetric assay for cell growth and survival: modifications to the tetrazolium dye procedure giving improved sensitivity and reliability, J. Immunol. Methods 89 (1986) 271–277.
[40] T. Mosmann, Rapid colorimetric assay for cellular growth and survival: application to proliferation and cytotoxicity assays, J. Immunol. Methods 65 (1983) 55–63.
[41] D.T. Vistica, P. Skehan, D. Scudiero, A. Monks, A. Pittman, M.R. Boyd, Tetrazolium-based assays for cellular viability: a critical examination of selected parameters affecting formazan production, Cancer Res. 51 (1991) 2515–2520.
[42] M.F. Tolba, A. Esmat, A.M. Al-Abd, S.S. Azab, A.E. Khalifa, H.A. Mosli, S.Z. Abdel-Rahman, A.B. Abdel-Naim, Caffeic acid phenethyl ester synergistically enhances docetaxel and paclitaxel cytotoxicity in prostate cancer cells, Int. Union Biochem. Mol. Biol. 65 (2013) 716–729.
[43] Protein Data Bank, http://www.rcsb.org/pdb.